



Analysis of sustainability metrics and application to the catalytic production of higher alcohols from ethanol



Akshay D. Patel^{a,*}, Selvedin Telalović^b, Johannes H. Bitter^{b,c}, Ernst Worrell^a, Martin K. Patel^{a,1}

^a Energy and Resources, Copernicus Institute of Sustainable Development, Utrecht University, Heidelberglaan 2, 3584 CS Utrecht, The Netherlands

^b Inorganic Chemistry and Catalysis, Utrecht University, 3508 TB Utrecht, The Netherlands

^c Biobased Commodity Chemistry, Wageningen University, 6700 AA Wageningen, The Netherlands

ARTICLE INFO

Article history:

Received 24 July 2013

Received in revised form 25 March 2014

Accepted 27 March 2014

Available online 10 June 2014

Keywords:

Sustainability analysis

Catalysis

Early-stage assessment

Guerbet reaction

2-Ethyl-1-hexanol

ABSTRACT

Use of sustainability metrics can help channel chemical research toward important long-term societal goals. For effective outcomes, it is important to understand the strengths and weaknesses of the sustainability assessment methods that can be applied in the chemical process development chain. In this paper we report the results from application of sustainability metrics in parallel with findings from laboratory research for production of higher alcohols from ethanol by application of the Guerbet reaction. 2-Ethyl-1-hexanol is used as an exemplary compound for the targeted higher alcohols. The accuracy of early-stage sustainability metrics using laboratory data is evaluated by comparing the results with metrics based on detailed process simulation models, techno-economic analysis and life cycle assessment. The analysis has provided insights on pitfalls to avoid and effective application of early-stage metrics considering the dynamic nature of information available from laboratory research. Anticipation of the process configuration was found to be particularly important for effective application of early-stage metrics. The results from catalysis research for 2-ethyl-1-hexanol highlight the potential opportunities for higher chain Guerbet alcohols from biobased ethanol. The comparison of this biobased route with conventional fossil based process shows the challenges for such a process from an economic and environmental perspective.

© 2014 Elsevier B.V. All rights reserved.

1. Introduction

Chemical research has been an important contributor to our societal progress. The future of this progress depends on harnessing the potential of chemical research to address crucial sustainability issues like resource depletion, global warming and affordable access to renewable resources. Hence it is imperative to supplement laboratory research with metrics which enable incorporation

of sustainability aspects in chemical process development, i.e. at early stage. Anastas' Twelve Principles of Green Chemistry [1] were a milestone in this respect and since then, there have been some developments toward quantitative operationalization of these principles [2,3]. The renewability of feedstocks is one of the core characteristics of a sustainable chemical process. Hence there has been increased research interest in the development of new routes to produce chemicals and fuels from biobased resources [4]. Continuing research and development efforts in this direction have resulted in the commercialization of renewables based chemical processes for production of ethanol, ethene, propylene glycol, butanol [5] among others. The production of these chemicals and fuels from biobased resources has been shown to offer environmental benefits like lower greenhouse gas emissions and non-renewable energy use [6–9]. However, continued progress on this path hinges on the development of novel inherently sustainable chemical processes which are optimized across economic, environmental and social parameters.

In the past decade, there has been a significant increase in the production of bioethanol [10] from first generation biobased feedstocks like corn and sugarcane. For the medium to long term, the production from lignocellulosic resources offers a potentially

Abbreviations: 2-EH, 2-ethyl-1-hexanol; TE, techno-economic; LCA, life cycle assessment; ESA, early stage assessment; EU, European Union; EUR, euros (currency); kg, kilogram; μm , micrometer; mL, milliliter; K, temperature in Kelvin; CNF, carbon nano-fibers; MgO, magnesium oxide; CaO, calcium oxide; BaO, barium oxide; MgAl, magnesium–aluminum; H₂, hydrogen gas; N₂, nitrogen gas; i.d., internal diameter; GC, gas chromatography; PM, physical mixture; EF, electricity factor; CHP, combined heat and power; GHG, greenhouse gases; CED, cumulative energy demand; NREU, non-renewable energy use; REU, renewable energy use; SIR, sustainability index ratio.

* Corresponding author. Tel.: +31 30 253 2081.

E-mail address: a.d.patel@uu.nl (A.D. Patel).

¹ Permanent address: Institute of Environmental Sciences and Forel Institute, University of Geneva, Geneva, Switzerland.

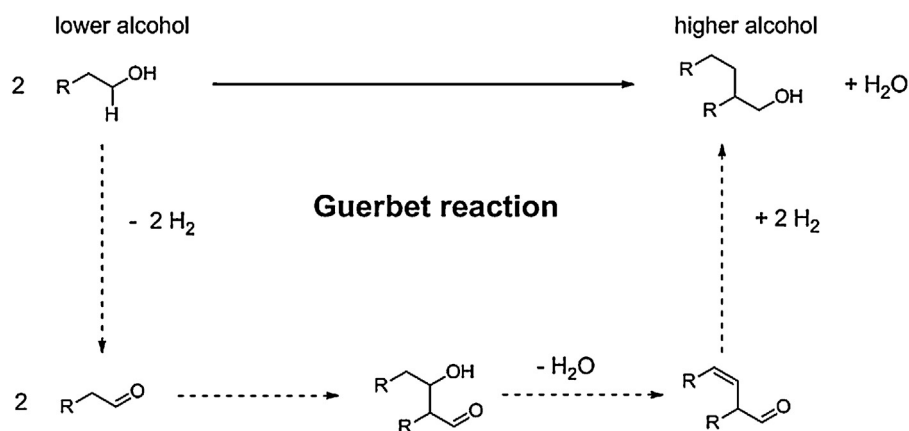


Fig. 1. Guerbet reaction represented as a sequence of four different reaction steps: dehydrogenation, aldol condensation, dehydration and hydrogenation.

more sustainable [11] and reliable supply of bioethanol. With these feedstock and chemical process developments, bioethanol is emerging as one of the key building blocks for production of renewable chemicals. This has led to identification of several conventionally produced chemicals for which production from bioethanol is an attractive alternative [12]. One such potentially interesting family of products is Guerbet alcohols which are widely used in the chemical industry for applications like cosmetics, chemical intermediates, lubricants and solvents [13,14]. The process of producing higher alcohols from ethanol via Guerbet reaction has already been known for over a century [15]. It is generally accepted that the Guerbet reaction is a sequence of different reactions starting from dehydrogenation of alcohol, followed by aldol condensation, dehydration and finally hydrogenation of the unsaturated aldehyde (Fig. 1). However, there have also been studies that claim a direct condensation of starting alcohol without intermediate aldol condensation step [16].

Depending on the starting alcohols the Guerbet alcohols are either linear or branched primary alcohols. One of the most widely known Guerbet alcohols is 2-ethyl-1-hexanol (2-EH) which is used primarily for the production of plasticizers (dioctylphthalate) and has a global market volume of 2.5 million metric tonne per year [17]. Industrially, homogeneous catalysts are applied to convert starting alcohols containing usually more than 6 carbon atoms toward Guerbet alcohols. Usually corrosive bases such as potassium hydroxide with or without the presence of a soluble metal complex are used. The water produced is continuously removed by the addition of a desiccant like CaO [18–22]. Apart from reliance on conventional fossil feedstocks, one other disadvantage of this approach is the corrosive nature of soluble bases used. This leads to high initial capital costs and high amounts of spent catalyst per tonne of product leading to increased requirements for wastewater treatment. Consequently 30% of the selling price is product purification and waste treatment [23]. Hence a potential solution, which is the target of current research, is to perform this reaction in gas phase utilizing a heterogeneous catalyst and bioethanol as starting alcohol. There are several examples in the literature that utilize heterogeneous catalysts, mainly for the Guerbet conversion of ethanol to 1-butanol. Catalysts used are mainly MgO, MgAl mixed oxides and hydroxyapatites. A good review of applied heterogeneous catalysts for ethanol condensation toward 1-butanol is given by Kozłowski [24]. In our research we used alkaline earth metal oxide nanoparticles of different base strength supported on carbon nano-fibers (CNF) as catalysts. CNF have a relatively high surface area ($\sim 150 \text{ m}^2 \text{ g}^{-1}$) and are inert and therefore suitable as catalyst support under demanding conditions. Simple base oxides are capable of, next to performing the aldol reaction, conducting

dehydrogenation/hydrogenation reactions (first and last step of Guerbet reaction, see Fig. 1). For the latter steps often high temperatures are required with these catalysts rendering the catalytic system less sustainable in terms of energy consumption [25]. A possible solution to decrease the amount of energy required, i.e. by lowering the reaction temperature is to add a metal function to the basic oxide as metals are far more efficient dehydrogenation/hydrogenation catalysts [26]. More elaborate information on the current state of the art on heterogeneously catalyzed Guerbet reaction has been included in Appendix D1 [23,24,27–42].

In this article we use 2-ethyl-1-hexanol (2-EH) as a representative compound for higher Guerbet alcohols and report the application of different sustainability metrics in parallel with catalyst developments. We highlight the laboratory developments alongside stepwise sustainability analysis at different stages. Thus, we present the advances in catalytic research and also analyze the accuracy of the early-stage sustainability assessment method and explore how it could be improved. Accordingly the following facets are covered in this study:

- (1) Laboratory developments for Guerbet alcohols.
- (2) Primary early-stage sustainability assessment (primary ESA) at the onset of laboratory research.
- (3) Detailed analysis based on process design, techno-economic (TE) analysis and life cycle assessment (LCA) for 2-EH as an example for Guerbet alcohols.
- (4) Updated early-stage sustainability assessment (updated ESA) based on new insights gained in process design.

An important aim of this research is to bring together quantitative sustainability assessment methods and laboratory research to enable effective development of sustainable chemical processes. Using very early stage information and results at the onset of this chemical research, sustainability assessments for nine processes were performed [43] based on the methodology reported in Patel et al. [2]. One of these early-stage analyses was based on a one reactor approach for the production of 2-EH from ethanol and helped to highlight the potential benefits and drawbacks of this process. The assessment indicated that a biobased process would be potentially favorable. Following this first assessment, we present in this paper a more detailed analysis that was performed with techno-economic (TE) analysis and life cycle assessment (LCA), based on a conceptual process simulation model. In the course of process model development it was found that instead of one reactor, a scheme involving four reactors is more feasible for this process which was therefore the basis for the simulation model (including economic assessment and LCA). Considering the change in lay-out,

a new early-stage analysis according to Patel et al. [2] was performed for a four-stage reactor configuration which relied on the new insights gained during detailed assessment. We then investigate the conformity of results obtained from the different early stage analyses and the detailed analysis. This has enabled us to identify the suitability of early stage analysis, pinpoint the sources of differences in the outcomes compared to detailed analysis and provide guidance for future assessments. This study highlights the learning realized by making use of the results of the experimental research for assessment activities which, in turn, allowed to take informed decisions for the next round of experiments. This learning is demonstrated by the progress in the catalyst development and assessment approaches. Thus in this article we present the results for laboratory developments, two variants of early stage assessment and for prospective techno-economic and life cycle assessment for the production of 2-EH.

2. Materials and methods

This study involves a combination of laboratory experiments and analytical models. In this section we present the methods and key assumptions that underpin each of the four facets of this study as listed earlier in the introduction. Appendix A lists some of the key data inputs common across all the facets of this study.

2.1. Laboratory developments for Guerbet alcohols

2.1.1. Materials and reagents

All reagents were used as received. Magnesium nitrate hexahydrate, 99+%, for analysis and copper(II) nitrate trihydrate, 99%, pro-analysis were acquired from Acros. Barium nitrate, ACS reagent, ≥99%, was acquired from Sigma–Aldrich. Oxidized CNF (oxidizing agent HNO_3) was used as support and was prepared as described elsewhere using Ni/SiO_2 as growth catalyst [44–46].

2.1.2. Catalyst preparation

Supported base (alkaline earth) catalysts were prepared by incipient wetness impregnation using aqueous solutions of the corresponding nitrates on oxidized CNF (425–212 μm). All samples contained the same molar metaloxide loading (1.5 mol%). After impregnation the samples were dried under dynamic vacuum at RT and stored under inert atmosphere.

Cu-MgO/CNF was prepared by co-impregnation of an aqueous solution of Mg-nitrate and Cu-nitrate . The MgO (MgO 1.5 mol%) to Cu ratio was varied from 10 to 30 thereby resulting in different weight percentage of copper (0.27, 0.41 and 0.82). A sample containing only copper (Cu/CNF , 0.82 weight percentage of copper) was also synthesized by incipient wetness impregnation using copper nitrate.

The alkaline earth metal oxides (AEMO) were activated at 600 °C (ramp 5 °C min^{-1} , dwell 3 h) in N_2 (30 ml min^{-1}). In case Cu was present this treatment was followed by a reduction step (350 °C, ramp 5 °C min^{-1} , dwell 5 h) in N_2/H_2 (2/1, 30 ml min^{-1}). After activation the catalysts were stored under inert atmosphere before further use. In case Cu/CNF was synthesized without the presence of base, this catalyst was directly reduced without prior activation step (350 °C, ramp 5 °C min^{-1} , dwell 5 h in N_2/H_2 (2/1, 30 ml min^{-1})).

2.1.3. Characterization techniques applied

The crystallinity and particle size of the catalysts were characterized using a Bruker D8 Advance XRD with $\text{Co K}\alpha$ radiation ($\lambda = 1.789 \text{ \AA}$). The basicity of the samples assessed using CO_2 chemisorption was performed on a Micromeritics ASAP 2020 V4.00 system. The samples, previously activated at 600 °C under nitrogen

for 3 h were loaded in the reactor in a glove box. CO_2 adsorption measurements were performed at 0 °C. Adsorption isotherms were obtained by plotting CO_2 uptake versus absolute pressure. By extrapolating the linear part of the isotherm to zero bar pressure the total number of basic sites was determined.

N_2 physisorption measurements were carried out using a Micromeritics TriStar 3000 V6.08 A system at –196 °C to determine BET surface area and pore volume ($p/p_0 = 0.96$).

TEM analysis of the samples was performed with an FEI Tecnai 12 an FEI Technai 20 F. The samples were placed on a holey carbon grid, and both bright field and dark field TEM images were recorded. Characterization results are provided in Appendix D1.

2.1.4. Catalyst testing

The catalysts were tested for the Guerbet reaction starting from ethanol ($T = 300 \text{ °C}$, using 200 mg of catalyst weighed under inert atmosphere). A plug flow quartz reactor with a 4 mm i.d. was used. Before testing the catalyst was heated to the reaction temperature in inert atmosphere (N_2) and kept at that temperature under static conditions for 5 h. In parallel the ethanol and propane (internal standard) flow was adjusted and stabilized. Subsequently that stabilized mixture was introduced to the reactor. Ethanol was supplied by means of a HPLC pump (9 $\mu\text{l min}^{-1}$) into a flow of 30 (ml min^{-1}) N_2 (containing 1.67 mol% propane as internal standard) through heat traced stainless steel tubing kept at 177 °C. This results in an 11 vol% ethanol feed stream. Contact time in ethanol was 5.6 s or 2 h^{-1} WHSV.

For the test with a physical mixture 0.5 g MgO/CNF and 0.2 g Cu/CNF were used (activated as described above for Cu-MgO/CNF). The reaction using this physical mixture was conducted at 200 °C with a contact time in ethanol of 18.3 s while the other conditions were the same as mentioned above. The physical mixture was compared to MgO/CNF also tested at 200 °C and a contact time in ethanol of 18.3 s.

The conversion is calculated based on the GC areas of ethanol ($A_{\text{ethanol,in}}$) and the internal standard propane ($A_{\text{propane,in}}$) determined before the reaction and area of ethanol and internal standard during the reaction ($A_{\text{ethanol,out}}$, $A_{\text{propane,out}}$):

$$\text{Conv}(\%) = \frac{(A_{\text{ethanol,in}}/A_{\text{propane,in}}) - (A_{\text{ethanol,out}}/A_{\text{propane,out}})}{A_{\text{ethanol,in}}/A_{\text{propane,in}}} \quad (1)$$

Selectivities are defined as the GC area of the product 'i' as a fraction of the total GC area of all products that are formed.

$$\text{Sel}(\%) = \frac{A_i}{\sum_{i=0}^n A_n} \times 100\% \quad (2)$$

Productivity is defined as:

$$\text{Productivity} = \frac{\text{Ethanol}_{\text{in}} (\text{mmol/h}) \times \text{Conv}(\%) \times \text{Sel}(\%)}{g_{\text{catalyst}}} \quad (3)$$

2.2. Primary early stage sustainability assessment (primary ESA)

The Primary early-stage sustainability assessment (primary ESA) was based on the methodology reported in Patel et al. [2] which makes use of information from laboratory research like reaction yields, concentrations and reaction temperature. The methodology compares the performance of a novel chemical process with a conventional process as a reference. In this paper, only the environmental and economic aspects of this methodology (pillars 1–3²) have been used to ensure a fair comparison with TE and LCA based detailed assessments. The categories and respective weighing factors (numbers associated with arrows) used for

² Refers to the 5 pillars (indicators) as described in the methodology article.

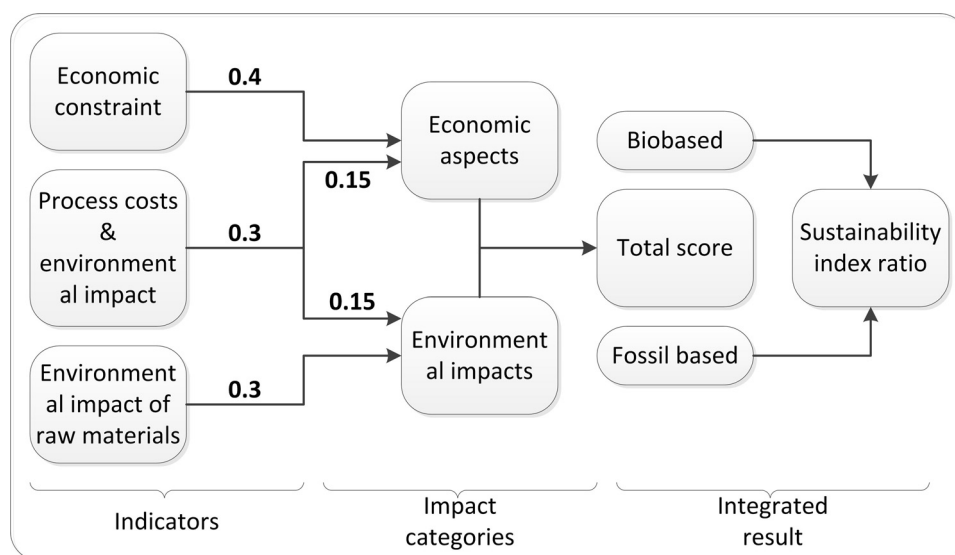


Fig. 2. Overview of early stage assessment methodology for integrated sustainability assessment (values represent weighting factors).

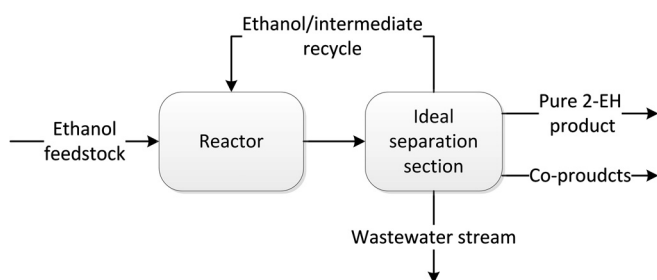


Fig. 3. Biobased process schematic for primary early stage assessment (primary ESA).

the purpose of this analysis are represented in Fig. 2. Consequently the economic aspects and environmental impacts have an effective weighting factor of 0.55 and 0.45 respectively in the integrated total score. As the indicators used are impacts, the lowest possible total score is aimed for. The sustainability index ratio (SIR) is the ratio of the total score of the biobased process to that of the fossil based process. Thus a SIR of less than '1' indicates that the biobased process is more favorable. Please refer to Appendix B for more information regarding the reasoning behind the weights and calculations based on this methodology.

The primary ESA was performed at the onset of the project based on the limited information for the biobased process available from laboratory experiments and assumptions at that time. This primary assessment which is based on a one-reactor approach has been reported under a different set of assumptions and data inputs in Patel et al. [2]. Based on the methodology, the early stage assessment analyzes a potential future process case with a one reactor system and a potentially ideal separation system³ which would lead to the final 2-EH product. It is envisioned that all the unreacted raw materials and the intermediate alcohols and aldehydes are recycled back to the reactor for further conversion to higher alcohols. Fig. 3 gives a schematic of the process configuration which formed the basis of the assessment. The relevant assumptions and mass balance data which form the basis of this assessment can be found in Appendix C. Appendix also includes a description of the reference conventional fossil based process for production of 2-EH.

2.3. Detailed analysis

2.3.1. Analysis methodology

For the purpose of in-depth assessment, a process simulation model was developed for a prospective 2-EH production process from ethanol. This simulation was developed using ASPEN Plus process engineering software [47]. Pinch analysis [48] was used to estimate the optimal heat integration potential for this process design. The unit operations, for which it was impossible or impractical to implement heat integration in practice (e.g. temperature difference less than 10 K, cooling of compressors) have been excluded from the Pinch analysis. The process has been modeled and sized to convert 375,000 metric tonnes of bioethanol into 213,000 metric tonnes of 2-EH per year while operating for 8400 h per year. The processing capacity is based approximately on the expected output of Abengoa bioethanol production plant in Rotterdam [49]. The mass and energy balance simulation formed the basis of TE assessment. The economic feasibility assessment was based on equipment price data from the SCENT tool [50] and raw material price data from various sources [51–55]. The year of reference for the economic analysis is 2011. Hence, the chemical market prices used in this study refer to June 2011. A discounted cash flow analysis was performed following the methodology of NREL [56] to arrive at a minimum viable product price at a fixed 10% internal rate of return and a zero net present value. The ratio of this minimum viable price and the market price of 2-EH produced from fossil resources is used as an indicator for economic viability of the production process from ethanol. The mass and energy balances from the process simulation model also form the basis of LCA model for the biobased process. The LCA models for the biobased and the fossil based routes were prepared using SIMAPRO software [57] and is based on data from the Ecoinvent v2 database [57] and other literature sources [9,58,59]. The geographical scope for the production is a potential plant in the Rotterdam area of the Netherlands. This is used as a reference for location specific data like the electricity and natural gas supply mix. A natural gas based combined heat and power (CHP) unit with an overall efficiency of 72% and an electricity factor (EF) of 0.613⁴ [60] is assumed to provide the steam and electricity requirements for both the biobased and conventional

³ A separation system which completely separates out the unreacted raw materials for recycle, the products, the co-products and the waste stream.

⁴ The heat output of the CHP unit is $\{(1/(1+EF)) \times \text{input energy} \times \text{overall efficiency}\}$ and the remaining useful output is electricity.

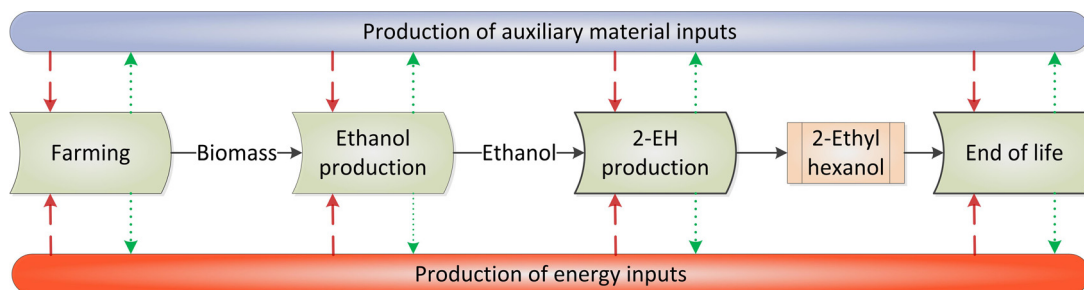


Fig. 4. System representation for biobased 2-EH.

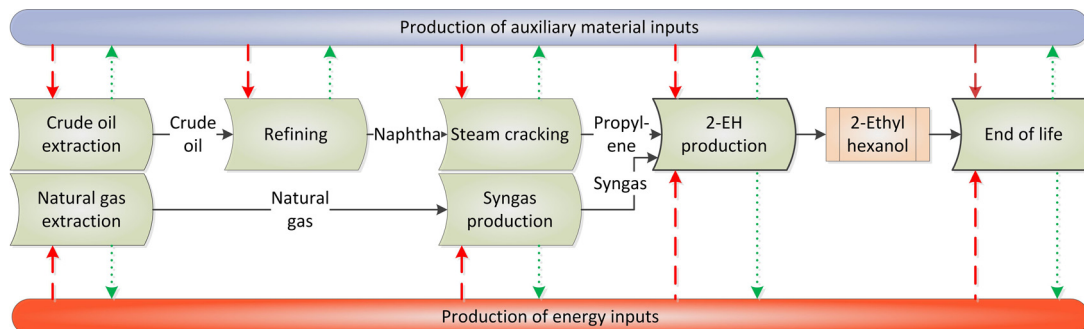


Fig. 5. System representation for fossil based 2-EH.

fossil based processes. It is also assumed that at the end of life, the energy contained in the product is recovered via waste incineration with an overall efficiency of 33% (11% as electricity and 22% as heat) based on lower heating value of the product [61]. Since the bio-based and the fossil based process lead to chemically identical products, the use phase⁵ is same for both the systems and hence is not considered for this comparative analysis. In contrast, end-of-life waste management has to be modeled due to the different origin of the carbon embodied in the final product (fossil versus bio-based). Figs. 4 and 5 show the system diagram for both the biobased and fossil based systems for 2-EH.

Climate change contribution (equivalent kg CO₂ units) based on greenhouse gas (GHG) emissions and cumulative energy demand (CED) are the two impact categories studied in the assessment. This choice was made to ensure consistency with the early stage assessment methodology and based on literature [62] information regarding the usefulness of these indicators. The calculation for climate change contribution is based on the IPCC GWP100 methodology [63] and the CED calculation is based on the methodology reported in Huijbregts et al. [62]. In line with the early stage assessment [2], we assume also for the detailed analysis that both the CED and GHG contribute equally to the environmental impact indicator. More specific information regarding the variety of data and assumptions used for economic analysis and life cycle assessment can be found in Appendix D section D3 and D4. It is acknowledged that more environmental impact categories would need to be taken into account for a complete environmental impact assessment (compare [64]). As reported in Tufvesson et al. [65], inclusion of other environmental impacts apart from CED and the contribution to climate change offers a more complete understanding about the impacts associated with the chemical process. However, this

information should be included simultaneously in the early stage and detailed analysis in a consistent manner with appropriate indicators. Further studies are needed to pinpoint specific indicators and methods that will enable inclusion of such impacts without significantly increasing the data requirements for an early stage analysis.

Similar to early stage assessment, a sustainability index ratio (SIR) was calculated for the in-depth assessment following the methodology described by Fig. 6. The numbers associated with the arrows represent the weighting factors for economic and environmental impact categories, which are in-line with the weights of these categories for the early stage assessment. Before applying the weighting factors, each of the indicators (price ratio, GHG and CED) is normalized internally (divided by the maximum value for biobased and fossil based). This ensures unit-less numbers which can be weighted and added to yield a total score. SIR is the ratio of the total score for the biobased process and the fossil based process; the method applied is identical for the early stage assessment and the in-depth assessment, allowing direct comparability.

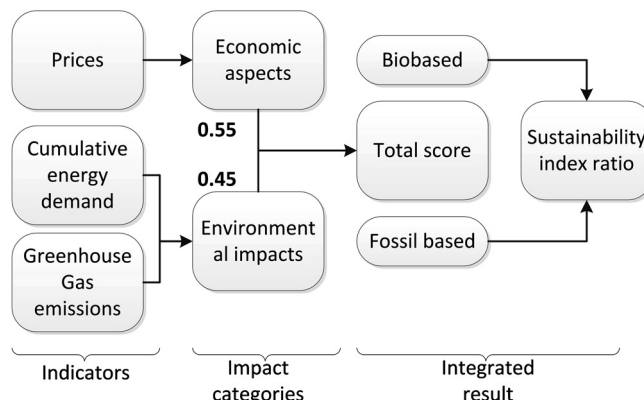


Fig. 6. Overview of integrated assessment based on detailed analysis.

⁵ Use phase includes the use of this chemical to further produce other chemicals which are transformed into products that are then used by the consumers and at the end of their useful life are discarded as waste. In this study we consider that this waste is incinerated thus leading to energy recovery and emissions at the end of life.

Table 1

Overview of reactions taking place in the process simulation for conversion of ethanol to 2-EH.

Reactor	Feed	Conversion (mol/mol)	Reaction	Selectivity
1	Ethanol	0.5	Ethanol \rightarrow Ethanal + H ₂	0.9
			Ethanol \rightarrow Ethene + H ₂ O	0.1
2	Ethanal Ethene	1	2*Ethanal + H ₂ \rightarrow 1-butanol + H ₂ O	1
			Ethene + H ₂ \rightarrow Ethane	1
3	1-Butanol	0.5	1-Butanol \rightarrow Butanal + H ₂	0.9
			1-Butanol \rightarrow Butene + H ₂ O	0.1
4	Butanal Butene	1	2*Butanal + H ₂ \rightarrow 2-EH + H ₂ O	1
			Butene + H ₂ \rightarrow Butane	1

2.3.2. Process description

The conversion of ethanol to 2-EH takes place via two Guerbet reactions. The first Guerbet reaction involves conversion of ethanol to 1-butanol which is subsequently converted to 2-EH in the second Guerbet reaction step (see Table 1). The Guerbet reaction takes place via dehydrogenation to aldehydes and hydro-condensation (involving aldol condensation, followed by dehydration and finally hydrogenation reactions to higher alcohols). Hence, contrary to the assumption of one single reactor according to the primary ESA (see Fig. 2), it was found that the Guerbet reaction should be preferably carried out in two reactors. The first reaction can be carried out in the gas phase in a dehydrogenation reactor operating at low pressure to shift equilibrium toward the formation of aldehydes and hydrogen. The second high pressure hydro-condensation reactor would favor the subsequent aldol condensation and hydrogenation reaction steps. To ensure lower by-product formation and higher yields in conversion of ethanol to 2-EH, we decided to use a four reactor configuration. In this configuration the first two reactors convert ethanol to 1-butanol and the subsequent two reactors

convert purified 1-butanol to 2-EH (see Table 1). Section D2 in Appendix includes more information on the reasoning behind a four reactor approach. Fig. 7 shows the process flow diagram for the simulation. The process is divided into seven sections as indicated in the figure. It is assumed that the required utilities (electricity, heating, cooling and waste treatment) are purchased from outside the battery limits. The aim of the analysis is to assess a best case future scenario for this reaction scheme, hence high yields are assumed. Table 1 gives the conversions and selectivities for the various reactions modeled in the four reactors. Additional detailed description of the process model and assumptions can be found in Appendix D.

2.3.3. Updated early stage assessment (updated ESA)

The assumption of only one reactor according to the primary ESA was modified once the detailed process design had been developed. Hence, an updated ESA was carried out based on the process model assumptions to study the change in results of ESA. This updated ESA was based on a four reactor configuration and is represented in Fig. 8. The assumptions regarding the reactions are same as the ones for process model, while those for the separation sequence and subsequent evaluation are based on the methodology as described in the earlier section on primary ESA.

3. Results and discussion

In this section we first present the results from laboratory research on catalyst development. Thereafter we put these results into a broader perspective by providing findings and a discussion for each of the three sustainability assessment facets of this study. Subsequently the results from these three facets are compared to understand the applicability of the assessment methods and to identify the preferred approach offering practically usable and reliable metrics for process development at the laboratory stage.

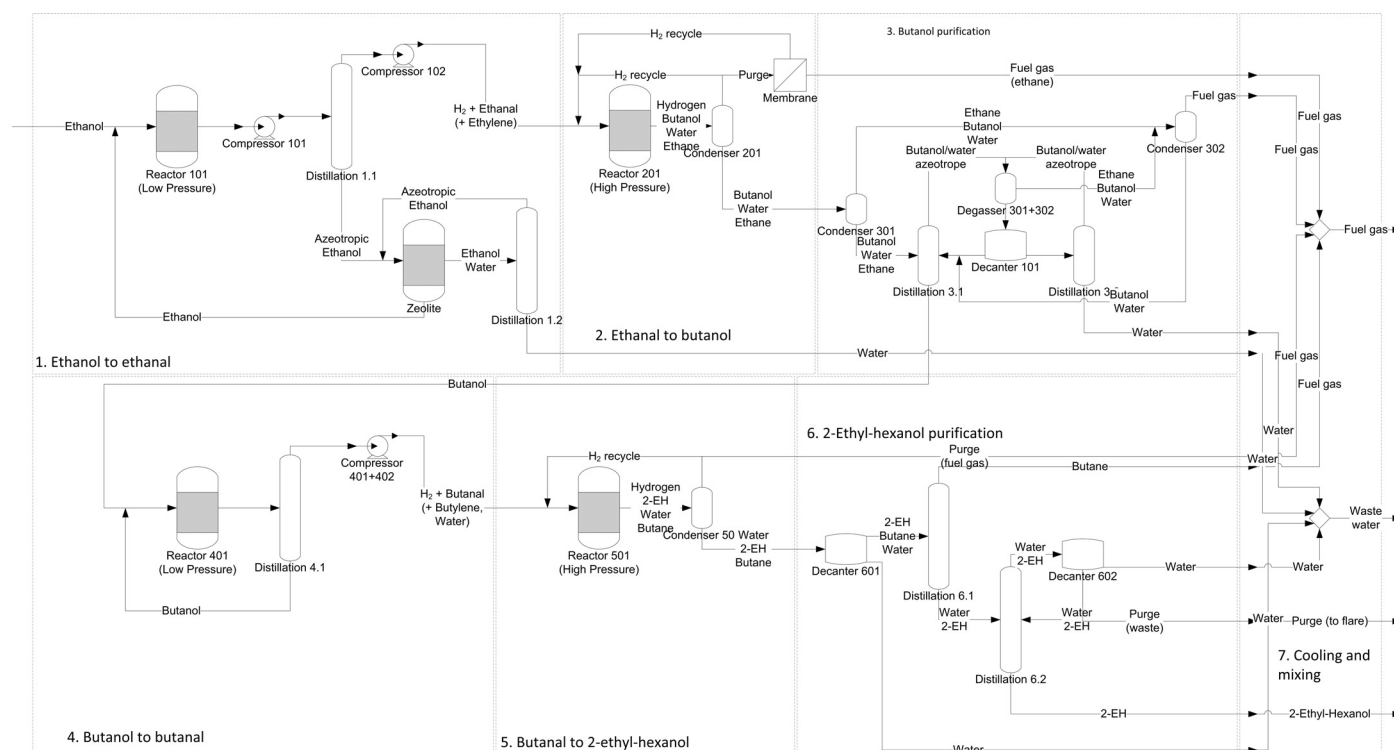


Fig. 7. Process flow diagram for production of 2-EH from biobased ethanol.

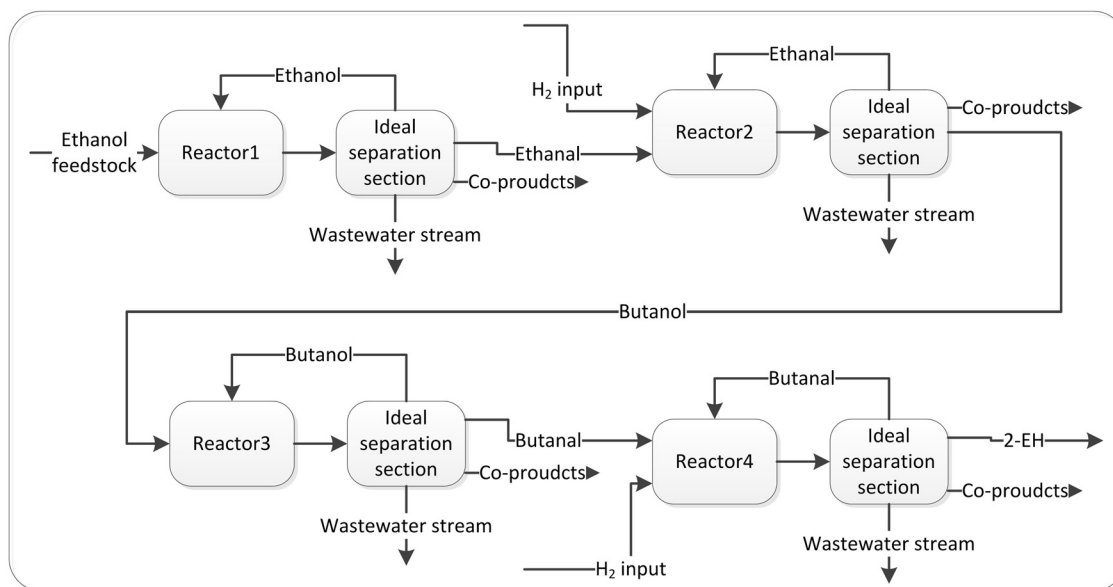


Fig. 8. Biobased process schematic for updated early stage assessment.

3.1. Laboratory developments for Guerbet alcohols

Fig. 9 displays the selectivities obtained (conversion levels plotted in Fig. 10) over two catalysts after 1 min (MgO and BaO) and 1 h time on stream (MgO-1h and BaO-1h). These selectivities are obtained with similar mol% of MgO and BaO supported on CNF. In general, the main products obtained were ethanol and 1-butanol. Clearly the simple alkaline earth metal oxides alone are capable of catalyzing all the consecutive steps of Guerbet reaction including dehydrogenation/hydrogenation steps at 300 °C. Fig. 9 also shows that increasing basicity of the corresponding alkaline earth metal oxides (BaO having higher basicity than MgO) leads to increased production of higher alcohols such as 2-ethyl-1-hexanol and 1-octanol in the case of BaO after 1 min of reaction. In case of MgO after 1 min of reaction time the highest alcohol obtained is 1-hexanol. After 1 h of reaction time (bars MgO-1h and BaO-1h) the highest alcohol obtained with MgO was 1-butanol and in the case of BaO it was 1-hexanol.

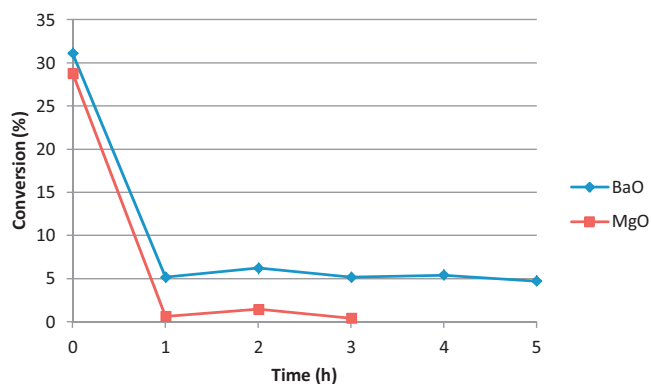


Fig. 10. Conversions over time obtained using MgO and BaO supported on CNF, tested at 300 °C, using 200 mg of catalyst, 11 vol% ethanol, and contact time of 5 s.

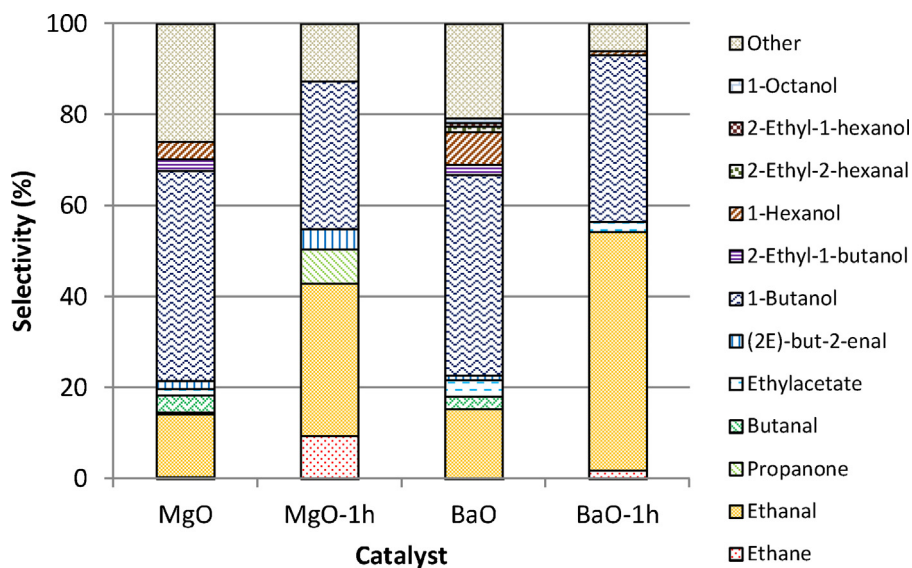


Fig. 9. Selectivities obtained with MgO and BaO nanoparticles supported on CNF with same mol% tested at 300 °C, using 200 mg of catalyst, 11 vol% ethanol, and contact time of 5 s. Associated data values are provided in Appendix F.

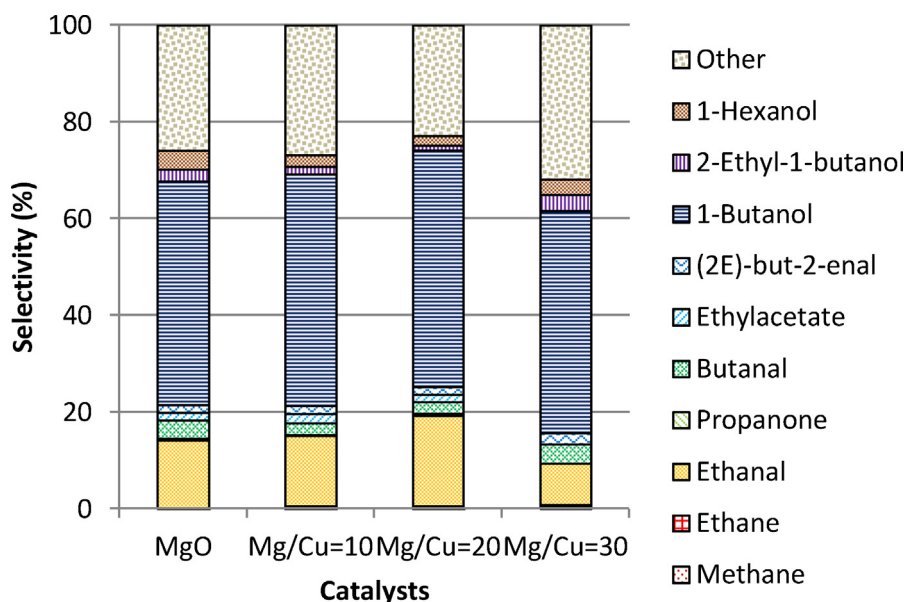


Fig. 11. Selectivity of bi-functional copper-magnesium oxide catalysts supported on carbon nanofibers and tested at 300 °C, using 200 mg of catalyst, 11 vol% ethanol, and contact time of 5 s. Associated data values are provided in [Appendix F](#).

[Fig. 10](#) displays the ethanol conversion as function of time over MgO and BaO catalysts whose selectivities are depicted in [Fig. 9](#). Clearly both catalysts lost a significant part of their activity during the first hour time on stream, from around 30% ethanol conversion to 1% in case of MgO and 5% in case of BaO. Nevertheless BaO retains a low but significant activity (5%) after that.

To increase the activity of supported alkaline earth metal oxides we added a metal (Cu) to MgO (MgO was chosen since it the best available and more sustainable alkaline earth metal oxide) as metals are much better dehydrogenation/hydrogenation catalysts than oxides [26]. Cu was chosen as dehydrogenation/hydrogenation catalyst based on our catalytic results (not shown) where Cu alone supported on CNF was highly selective toward ethanal production from ethanol.

[Fig. 11](#) shows selectivities obtained with different Cu/MgO/CNF (Mg/Cu = 10, 20, 30 and pure MgO/CNF) catalysts after 1 min time on stream. All catalysts contain the same mol% of MgO. [Fig. 11](#) shows that adding a metal (Cu) by impregnation to MgO did not have a significant influence on the selectivity of the reaction. Also ethanol conversions were not affected by addition of Cu by impregnation (results not shown).

Better results were obtained by using a physical mixture of copper and magnesium oxide, both supported on CNF. In this case the catalysts were tested at 200 °C. The lower temperature was chosen based on the fact that fast deactivation of Cu alone supported on CNF during ethanol conversion at 300 °C was observed. Initial conversion dropped in that case from 90% to less than 5% within 4 h reaction time, ethanal being the main product formed. In addition, alkaline earth metal oxides supported on CNF are capable of

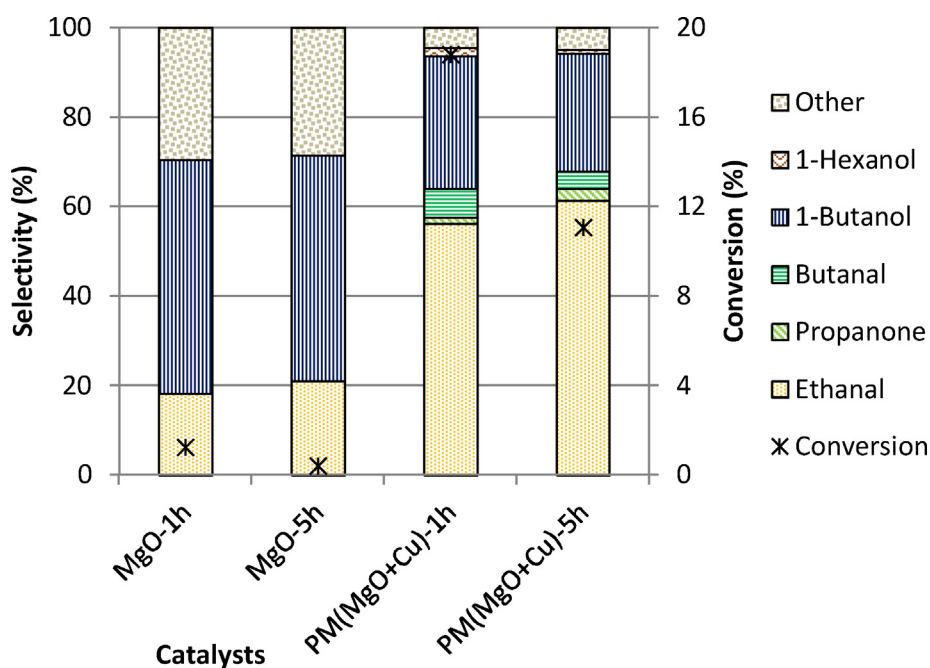


Fig. 12. Selectivities and conversions of physical mixtures of MgO/CNF and Cu/CNF tested at 200 °C and compared to MgO/CNF at the same temperature at 1 h and 5 h reaction time, using 500 mg MgO/CNF and 200 mg Cu/CNF, 11 vol% ethanol and contact time of 18.3 s. Associated data values are provided in [Appendix F](#).

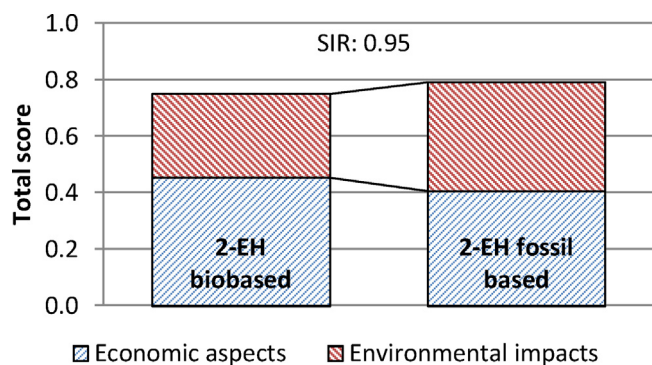


Fig. 13. Comparative integrated results for primary ESA of biobased and fossil based 2-EH.

conducting aldol reaction (one of the steps in the overall reaction scheme (Fig. 1) at even lower temperatures than 200 °C. For example, propanone aldol condensation using alkaline earth metal oxides supported on CNF is conducted at a temperature of around 0 °C [66].

In Fig. 12 selectivities obtained at a reaction temperature of 200 °C and different reaction times (1 and 5 h) are depicted for MgO/CNF and physical mixture (PM) of MgO/CNF and Cu/CNF (PM (MgO + Cu)) both supported separately on CNF. In this graph the conversions obtained are also displayed (secondary axis). MgO/CNF alone showed low conversion of only 1% due to its low dehydrogenation/hydrogenation abilities at this low temperature. Addition of Cu/CNF to MgO/CNF, thus making a physical mixture, greatly increased conversion of ethanol (Fig. 12). After 5 h on stream the physical mixture of MgO/CNF and Cu/CNF showed an ethanol conversion of 12% while MgO/CNF was barely active at all.

MgO/CNF was more selective toward 1-butanol than the physical mixture of MgO/CNF and Cu/CNF which showed the highest selectivity toward ethanol followed by 1-butanol. In case of the physical mixture also 1-hexanol was obtained which was not seen in case of MgO/CNF.

Based on conversions and selectivity's obtained in Fig. 12, in case of physical mixture productivity of 1-butanol was around 8 times higher than if MgO/CNF alone was used at reaction temperatures of 200 °C (0.74 mmol_{1-butanol}/hg_{catalyst} for PM (MgO + Cu) and 0.09 mmol_{1-butanol}/hg_{catalyst} for MgO/CNF at *t* = 1 h). Addition of copper, an effective dehydrogenation/hydrogenation catalysts confirms the notion that oxides, in this case alkaline earth metal oxides, are not efficient dehydrogenation/hydrogenation catalysts as they are efficient aldol condensation catalysts.

Irrespective of the base strength of alkaline earth metal oxide (MgO vs BaO) or addition of a metal function (Cu) to the base catalyst, the main alcohol formed from ethanol was always 1-butanol. Thus, applying heterogeneous catalysis for the synthesis of 2-ethyl-1-hexanol based on literature study and own catalytic results at least two reactors are needed. In the first reactor ethanol is converted to 1-butanol and in the second reactor 1-butanol is converted to 2-ethyl-1-hexanol. However, based on process design, a four reactor approach would enable use of more selective catalysts in conditions favorable for the reactions, which can reduce the formation of by-products and lead to higher yields for specific higher alcohols like 2-ethyl-1-hexanol.

3.2. Primary early stage assessment

Fig. 13 shows the integrated result of the primary ESA. With a sustainability index ratio (SIR⁶) of 0.95, the figure shows that

Table 2

Mass balance for production of 2-EH from biobased ethanol.

Stream	Component	Flow (metric tons per year)
Input	Ethanol	375,000
	Hydrogen	2400
Output	2-Ethyl-1-hexanol	213,000
	Wastewater (0.1 wt% organics)	117,000
	Fuel gas (ethane, butane)	46,000
	Waste gas (to flare)	1200

Table 3

Utility requirements for production of 2-EH from biobased ethanol.

	Heating (MJ/kg 2-EH)	Cooling (MJ/kg 2-EH)	Electricity (MJ/kg 2-EH)
No heat integration	27.9	28.7	2.2
Optimal heat integration	13.3	14.0	2.2 ^a

^a Electricity use remains the same as the analysis is based on process flow design model. The changes would be observed in a detailed piping and instrumentation design.

subject to relevant assumptions, the biobased process can be beneficial as compared to the fossil based process. The marginally higher economic benefits of the fossil based process are negated by the higher expected environmental impacts. Thus an ethanol based process which progressively cycles intermediates to higher alcohols in one single reactor can seem to be an attractive option. However, it is important to note that this outcome does not take into consideration viability of the assumptions regarding catalyst and process performance along with other uncertainties such as prices of commodities. Also contrary to the analysis reported in Patel et al. [2] this analysis does not take into account EHS (Environment, Health and Safety) aspects which would be important to consider when assessing a chemical process. This has been done to ensure consistency with the detailed analysis. To analyze EHS aspects, process simulation information about the conventional process would also be needed which is not available.

3.3. Detailed analysis

Table 2 shows the mass balance results of the process simulation model for the biobased process for production of 2-EH from ethanol.

The overall modeled selectivity of ethanol to 2-EH is 80.5% on a carbon mole basis (i.e. 80.5% of the theoretical maximum). The majority of the mass losses occur in the two low pressure reactors along with some minor losses (1%) in the separation steps. Table 3 shows the total energy requirements for the process with and without heat integration. It can be observed that the heating and cooling requirements can be reduced by over 50% through heat exchange.

Table 4 provides a summary of the economic analysis results for this process. The minimum viable price (MVP) for the biobased product is about 45% higher than the market price of 1.56 EUR/kg for fossil based 2-EH. Using an ethanol price of about 0.71 EUR/kg

Table 4

Results of economic analysis for production of 2-EH from biobased ethanol.

Parameter	Value	Units
Total capital investment	321.53	million euros
Feedstock (ethanol + hydrogen)	311.82	million euros per year
Utility costs	54.47	million euros per year
Other operating costs	124.39	million euros per year
Minimum viable price for 2-EH	2.27	EUR/kg 2-EH
Feedstock associated price ^a	1.48	EUR/kg 2-EH

^a Contribution of feedstock ethanol costs in the final minimum viable price for 2-EH.

⁶ Ratio of the total score of biobased process to that of the fossil based process.

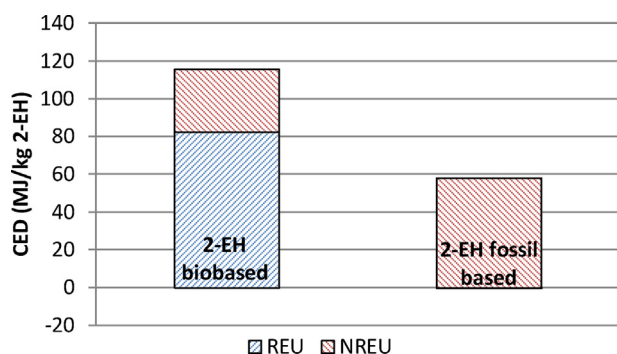


Fig. 14. Comparison of cumulative energy demand for biobased and fossil based systems for 2-EH.

in Brazil, the MVP for 2-EH at 2.08 EUR/kg is still about 33% higher than the market price. The MVP of the biobased product is sensitive to the price of feedstock ethanol and hydrogen which contribute 65% of the total MVP. Also for the fossil product, based on estimations for early stage assessment, the feedstocks contribute to approximately 65% of the market price. In the absence of an increase in the price of fossil based product, the price of ethanol has to drop to about 0.43 EUR/kg for the biobased product to achieve price parity. Following the NREL methodology for the analysis of process economics, 100% equity financing and modified accelerated cost recovery depreciation regime have been assumed. Instead, if 0% equity (and therefore loan financing at 8% interest rate for a 10 year time period) and straight line depreciation were chosen, then the results change only very marginally. The MVP of biobased product increases only by 2% (contribution of change in depreciation regime is only 0.06%) to 2.32 EUR/kg. As the price for biobased product is still about 48% higher (compared to 45% before) than the fossil based product, this would hence not influence the final conclusion. It should be noted that these results refer to a best case biobased process performance which assumes significant developments in catalyst research for this process.

Fig. 14 shows the results for the cumulative energy demand (CED) for the biobased and fossil based systems for 2-EH determined with the life cycle assessment model. In the figure the CED is shown as a sum of its two components, viz. renewable (REU) and non-renewable energy use (NREU). The biobased system has a higher CED as compared to the fossil based system. This is because

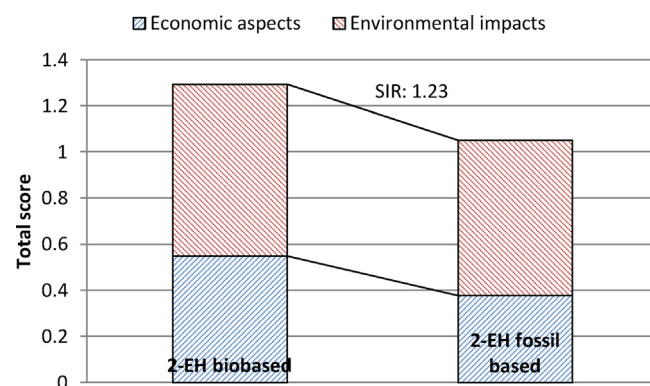


Fig. 16. Comparative integrated assessment results of biobased and fossil based systems for 2-EH.

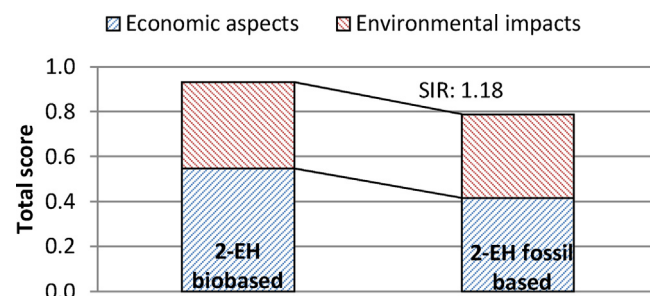


Fig. 17. Comparative integrated assessment results of updated ESA for biobased and fossil based 2-EH.

the fossil based system starts from liquid crude oil as compared to solid biomass and also it has been optimized through decades of process chain improvements. However, the biobased system entails about 40% lower NREU thus helping to reduce dependence on non-renewable resources. The CED as a whole is a proxy for a variety of environmental impacts [62] and hence reduction of CED is an important objective for further development of a biobased process system.

Fig. 15 shows the results for greenhouse gas emissions associated with the process systems. As can be observed the base case GHG emissions are about one-third lower for the biobased system compared to the fossil based system. The base case value will

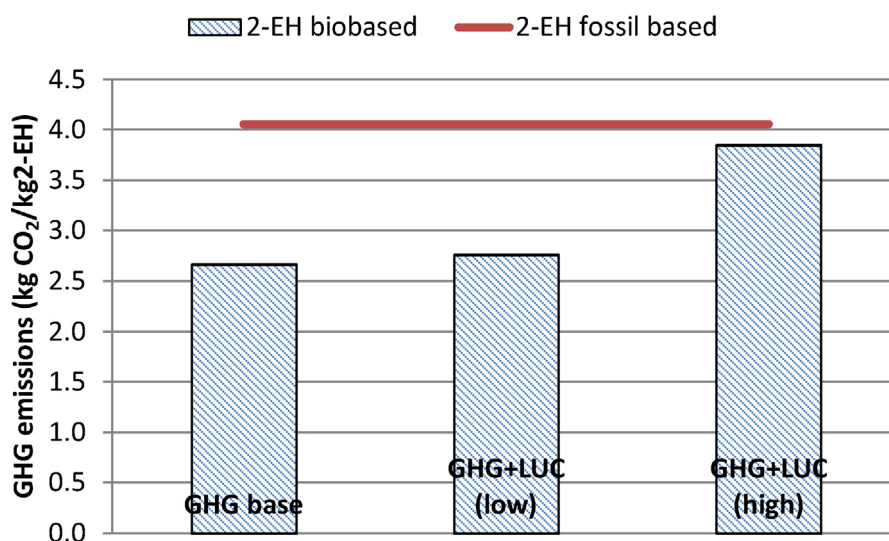


Fig. 15. Greenhouse gas emissions associated with biobased system for 2-EH including without and with additional impacts from land use change (low and high). Comparative greenhouse gas emissions for fossil based system for 2-EH.

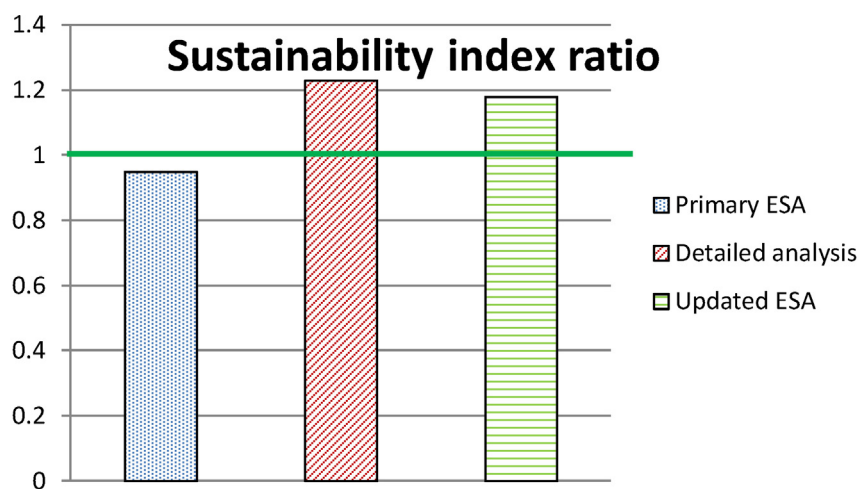


Fig. 18. Comparison of integrated assessment results for the three different analyses.

Table 5
Individual indicator results for updated early stage assessment.

Parameter	2-EH biobased	2-EH fossil based
Economic constraint (index)	0.89	0.65
Process costs and environmental impact (index)	6.60	5.59
Cumulative energy demand (MJ/kg 2-EH)	114.91	72.46
Greenhouse gas emissions (kgCO ₂ /kg 2-EH)	2.60	4.69

be used for the calculation of sustainability index ratio in the further course of this paper. A still debated, but potentially important aspect associated with biobased systems [67] is land use change. It entails that introduction of new biobased process systems leads to changes in conventional land use patterns (e.g. diversion of virgin forest or peat lands for agricultural use) which can lead to a net increase in greenhouse gas emissions. For the biomass system used in this study for ethanol production, the estimates for this increase range between 2 (low) and 25 (high) kg CO₂/GJ ethanol [68]. Hence the graph below also shows the effect of this uncertainty on the base case GHG emission estimate for the biobased process system.

Based on the above results for economic and environmental assessment, integrated results for the detailed analysis are shown in Fig. 16. Contrary to the primary ESA we now observe a SIR of 1.23 which indicates that the biobased system is not preferable compared to the fossil based system. The fossil based system scores better on the economic aspects as well as the overall environmental impact, considering the lower cumulative energy demand. However, this integrated outcome is also heavily dependent on the price, CED and GHG emissions associated with the bioethanol feedstock. Ethanol production from different systems like Brazilian production or lignocellulosic resource based production could lead to a lower overall SIR of 1.01 and 0.78 respectively.⁷ The reduction in SIR is mainly due to lower GHG emissions associated with these two ethanol production systems. This analysis is based on comparable assumptions, like combined heat and power based utilities, for both systems to ensure a fair comparison of metrics. However, in reality the fossil based systems with older technologies might

not necessarily have such upgrades, thus leading to higher environmental impacts. For example, the absence of a CHP unit for the fossil based system can lower the SIR from 1.23 to 1.17.

3.4. Updated early stage assessment

Table 5 shows the individual indicator results for the updated early stage assessment based on the four reactor design which was adopted considering the insights gained during the detailed process modeling. Since there was no change in the fossil based process data, the values for the fossil based 2-EH in updated ESA remain same as in the primary ESA. As can be observed the biobased process has higher scores (less preferable) for three of the four categories. Fig. 17 shows the integrated results for this updated ESA. With an SIR of 1.18 the ESA now indicates that the biobased process is less preferable as compared to the fossil based process.

3.5. Comparative analysis

Fig. 18 summarizes the outcome of the three analyses. As explained above, an SIR of more than '1' indicates that the biobased process is less preferable as compared to the fossil based counterpart and vice versa. The difference in primary ESA and the detailed analysis results are mainly due to the fact that the primary ESA was based on a one reactor model while the new insights gained in detailed analysis led to the implementation of a four reactor concept. The conformity of the detailed analysis results with updated ESA indicates the validity of the early stage assessment method. In the updated ESA the biobased process scores increased on all the three early-stage indicators viz. economic constraint, environmental impact of raw material and processing costs and environmental impacts. The reasons behind the specific choices made for primary ESA were the very limited amount of information available and more importantly, the lack of a process engineering perspective. Hence although the early stage assessment gives useful insights in the absence of a detailed process model, it is important that there is a good understanding of the principal design of the process already early on in the research. A variety of reaction and process information like reaction pathways, by-product formation and reaction energy are collected as a part of the early stage analysis. This information can also be used to develop an improved process layout. Such an approach can lead to a more informed early stage assessment which yields more accurate results and hence more specific guidance for catalyst development.

⁷ These are mainly provided as indicative scenarios based solely on different ethanol prices, CED and GHG emissions. [53,56,57,59] Ideally, these systems would be associated with different parameters for a range of other inputs which will be governed by the geographical location of the production systems.

4. Conclusion

In this study we have considered the developments of catalytic process toward production of Guerbet alcohols from biobased resources. This biobased process was analyzed using techno-economic and life cycle assessment based early stage and detailed metrics at different points in process development timeline.

Developments in the laboratory show that the alkaline earth oxide by itself can catalyze the Guerbet reaction, however, higher temperatures are needed which can lead to a higher energy demand. To lower the energy demand of the reaction, addition of a metal function to the alkaline earth oxides, gives better dehydrogenation/hydrogenation leading to much higher productivity than alkaline earth oxides. In addition, a bi-functional catalytic system can make it possible to apply a two reactor configuration for the production of 2-ethyl-1-hexanol from ethanol; however, for this approach a more extensive catalytic study would be required. For future research it is important to incorporate the metrics into laboratory research in an iterative approach for development of effective catalysts.

The detailed process analysis for a best case process performance scenario indicated that the biobased process might be less favorable than the fossil based process. However, this outcome depends on the feedstock parameters, system choices and market scenarios. Alternative feedstock choices indicate a comparatively better outcome for the biobased process. System choices like use of a combined heat and power units also affect the outcome. Also this analysis was carried out for a specific Guerbet alcohol (2-EH). Different market scenarios and production systems for other higher alcohols will certainly play an important role. These should be investigated in future to provide specific catalyst development guidance for production of a variety of higher alcohols via biobased processes. From a methodological perspective inclusion of EHS aspects in future can add a new dimension to the analysis and provide additional information about the hazard aspects and their scalability from early-stage to detailed assessment. The integration approach used in this study can be used to incorporate such additional indicators. The same approach can also be applied for analysis of scaled up processes.

At the onset of the study an early stage assessment for a future scenario indicated a potentially favorable biobased process. However, this was found to be at odds with the results from detailed analysis which was based on process design, techno-economic analysis and life cycle assessment.

This difference mainly emanated from the uninformed choices which were made at the onset of the analysis. As demonstrated by the updated early stage assessment the underlying methodology led to similar findings as those from the detailed analysis. This strongly indicates the validity of the methodology proposed for early stage assessment.

Hence, although the early stage assessment cannot be a replacement for detailed process analysis, it can certainly provide a quick scanning metric for development of more sustainable chemical processes. According to this case study the main challenge of the early stage assessment is to properly anticipate the reactor configuration. Collaboration with experienced process engineers and better use of the information collected during early stage analysis could make this task more feasible.

Nonetheless it is important to recognize that sustainability is a complex subject, which makes it necessary to further improve the early stage assessment methodology to improve its predictive power while incorporating more diverse economic, environmental and social impacts. With increasing sustainability challenges and emergence of a wide variety of potentially interesting solutions, such quick analysis metrics can help to effectively utilize both human and natural capital to enable a sustainable future.

Acknowledgements

We would like to acknowledge the valuable contribution of Raimo van der Linden, Herman den Uil, Ruud Grisel and Jaap van Hal from the Energy research Center of the Netherlands for this study. This research was funded by the SmartMix program of the Dutch government via the CatchBio (SSM06017) research project.

Appendix A.

Key data inputs and assumptions which remain uniform across all the three analytical facets of this study are provided in this section.

Table A1 provides information about the cumulative energy demand and greenhouse gas emissions associated with the production of various components used in this study along with the market price for the applicable components. Some cells are left blank as the specific data has not been used for this analysis.

Appendix B.

This section includes the calculations for early stage assessment methodology.

The following indicators from the early stage assessment methodology reported in Patel et al. [2] are used in this study. Together they integrate information regarding the life cycle of the process under consideration.

- Economic constraint (EC): This is the ratio of feedstock cost in the product price to that of the market price of the product.
- Process costs and environmental impact (PCEI): An indicator of the economic costs and the environmental impacts associated with the process.
- Environmental impact of raw materials (EI): An indicator for the life cycle environmental impacts based on feedstock consumption. The CED and GHG emissions are the two impact categories included in this indicator.

The calculation of integrated scores based on the overview provided in Fig. 2 in the article, is presented below. Considering that in today's market driven economy, a process has to be economically feasible to be practically implemented; the economic aspects have been given a higher weight (0.55) as compared to the environmental impacts (0.45). However, the difference between the two is relatively small considering the fact that economic prices, more or less represent current situation, while the environmental impacts bring in long term sustainability issues like depletion of resources and climate change among others. The 0.55 effective weight of the economic aspects is the sum of the 0.4 weight of economic constraint and half the 0.3 weight for PCEI indicator ($0.3/2 = 0.15$). Similarly the effective weight of environmental impacts is 0.45, 0.3 from EI and 0.15 from PCEI.

$$\text{Economic aspects} = (\text{EC}) \times [\text{weight} = 0.4] + (\text{PCEI}) \times [\text{weight} = 0.15]$$

$$\text{Environmental impacts} = (\text{EI}) \times [\text{weight} = 0.3] + (\text{PCEI}) \times [\text{weight} = 0.15]$$

$$\text{Total score for biobased process (Tb)} = \text{economic aspects score} + \text{environmental impact score}$$

$$\text{Total score for biobased process (Tf)} = \text{economic aspects score} + \text{environmental impact score}$$

$$\text{Sustainability index ratio (SIR)} = \text{Tb/Tf}$$

Appendix C.

This section includes the assumptions and mass balance data for primary ESA of 2-EH production process from biobased and fossil based resources.

As discussed in the article, the primary assessment is comparison of the biobased and the conventional fossil based process. A detailed description of the process, data and the relevant assumptions for both the biobased (at the primary stage) and fossil process for 2-EH is provided in this section.

The biobased process as modeled at the onset of the research project is envisioned to start from 100% pure ethanol and proceed in a single reactor in which the lower intermediates are continuously recycled until we reach higher alcohols (2-EH). Hence, after complete recycle, 2-EH and heavies (represented by dodecanol) are the main products from the process. However, still the 2-EH needs to be separated out from all the intermediates after the reactor step. Considering that this analysis relies on a potential future process case, the laboratory results were transformed with assumptions for upcycling of intermediate aldehydes and lower alcohols to 2-EH. In the 1 step experiment which has been shown in Section 2, several intermediates have been observed which in principle can lead to corresponding alcohols like 2-EH, butanol and hexanol on further reaction. Hence it is assumed that these alcohols will be the products from the process in addition to heavies (dodecanol is used as a proxy) and gases which are assumed to be ethene and butene. The reaction data reports a mass balance of 38% which documents the intermediate aldehydes and alcohols. An increase in the catalyst bed height was also observed after the reaction which indicates formation of heavies and presence of gases. Hence it is assumed that of the remaining 62% output, 40% goes to gases and 60% ends up in heavies. On an overall basis 80% of the converted ethanol

(50% conversion) is assumed to end up in liquids and solids and the remaining 20% ends up as gases. The selectivity for the fraction converted to liquids and solids is approximated from the observed reaction data and is assumed to be 0.3, 0.28, 0.12, 0.3 for 2-EH, butanol, hexanol and heavies respectively. It is also assumed that 80% of the gaseous product is ethene and the rest is butene and that 7% of the produced butanol and hexanol are converted to heavies after each recycle to produce 2-EH. It is assumed that heavies can be burned for process heat and hence a fuel value is assigned to them.

Based on these assumptions, an overview of the conversions and selectivities is as follows:

No. of steps: 1

Per pass conversion: 0.5 – refer to the assumptions below.

Overall selectivity: 0.38 – for 2-EH

Table A2 provides the mass balance data of the biobased process used for this assessment.

The fossil based process for production of 2-EH starts from propylene and syngas (2:1, H₂:CO) as raw materials and proceeds via hydrofomylation using rhodium, tri-phenylphosphine, sodium hydroxide as catalysts. This process is based on information from literature sources like Ullmann's Encyclopedia [17,69,70] and confidential commercial process information. It is a homogenously catalyzed process which takes place in 3 steps and proceeds via intermediate production of i-butanal and 2-ethylhexenal. As this process is based on existing data, the assessment model does not involve any major assumptions. The overview of the process is as follows:

Table A1
Key data inputs and assumptions.

Component	CED (MJ/kg, unless specified)	GHG (eq. kgCO ₂ /kg, unless specified)	Price (EUR/kg, unless specified)
Bioethanol – EU	70.7	1.47	0.82
Bioethanol – Brazil	75.1	0.34	0.71
Bioethanol – lignocellulosic	48.2	–0.29	0.68 ^a
Hydrogen	225	12.7	1.8
Propene	73.3	1.59	1.18
Syngas H ₂ :CO (2:1)	43.8	1.19	0.36
NaOH	45.6	2.2	0.46
2-Ethyl-1-hexanol			1.56
Iso-butanal			2.14
1-Butanal			1.02
n-Butanol			1.28
Butane			0.68
Natural gas			0.35
Hexanol			2.1
Butene			0.98
Ethene			1.19
Electricity production mix, Netherlands	3.07 (MJ/MJ)	0.186 (kgCO ₂ /MJ)	0.1 EUR/kWh
Water, decarbonized, at plant, RER	2.43E–5	7.75E–6	0.5 EUR/m ³
Water, completely softened, at plant, RER	2.95E–4	9.07E–5	1 EUR/m ³
Natural gas, high pressure, at consumer, RER	1.18 MJ/MJ	0.0114 MJ/MJ	7.5 EUR/GJ
n-Butanol	81	2.61	
Refinery gas	55.6	0.58	
Fuel oil	53.9	0.48	

References for the values presented above (also included in the main reference list).

[1] Pre Consultants, SimaPro-Ecoinvent database. 7.3 (2011).

[2] European Union, DIRECTIVE 2009/28/EC OF THE EUROPEAN PARLIAMENT AND OF THE COUNCIL of 23 April 2009 on the promotion of the use of energy from renewable sources and amending and subsequently repealing Directives 2001/77/EC and 2003/30/EC (2009).

[3] D. Mu, T. Seager, P. Rao, F. Zhao, Comparative life cycle assessment of lignocellulosic ethanol production: biochemical versus thermochemical conversion, Environ. Manag. 46 (2010) 565–578.

[4] ICIS, CW Price Reports, Chemical Week (2007–2011).

[5] Alibaba group, Chemicals (www.alibaba.com/Chemicals.p8), 2011 (2011).

[6] World Association of Beet and Cane Growers, Flashmarkets 2011 (2011).

[7] Dutch Association of Cost Engineers, DACE prijzenboekje, 28 ed., Dutch Association of Cost Engineers, Nijkerk, The Netherlands, 2011.

[8] Eurostat, Industrial gas prices for industrial consumers with annual consumptions between 10,000 and 100,000 GJ (2012).

^a This is not a market price and is based on NREL (included in references) study results and USD to EUR conversions.

Table A2

Mass balance data of the biobased process for primary ESA.

	Input	Output per pass	Overall output
Hydrogen	2.2	2.2	
1-Butanol	0.0	90.1	
2-EH	0.0	84.8	383.0
Heavies:dodecane	0.0	83.2	201.9
Ethanol	1000.0	500.0	
Hexanol	0.0	35.5	
Ethene	0.0	48.8	
Butene	0.0	12.2	
Water	0.0	147.7	295.3

Table A3

Mass balance data for fossil based process.

	Step-1		Step-2		Step-3	
	Input	Output	Input	Output	Input	Output
Propylene	809.0					
Syngas	577.0					
Triphenylphosphine	0.5	0.5				
Water	7071.6	7071.6	10.4	168.0		
n-Butanal		1301.8	1301.8			
i-Butanal		70.0				
Heavies:dodecanol		13.3				
NaOH			2.6			
2-Ethylhexenal				1103.2	1103.2	
Sodium butyrate				7.2		
Hydrogen				0.1	35.0	1.5
Butanol				12.2		
Butyric acid				15.1		
Butyl butyrate				9.0		
2-EH						1115.5
Butane						12.0
Methane						9.2

No. of steps: 3

Step-1: Per pass conversion: 1

Step-1: Selectivity: 0.94 – for n-butanol

Step-2: Per pass conversion: 1

Step-2: Selectivity: 0.97 – for 2-ethylhexenal

Step-3: Per pass conversion: 1

Step-3: Selectivity: 0.98 – for 2-EH

Table A3 provides a mass balance for the key components in this fossil based process.

Appendix D.

This section contains further information about the laboratory experiments, process simulation model, economic analysis model and the life cycle assessment model. The information pertains to reasoning behind specific choices, detailed process descriptions, assumptions and results. The references which are used in appendix are also included in the main list of references at the end of the article.

D.1. Guerbet reaction and laboratory experiments

Current state of heterogeneous Guerbet reaction

Even though solid bases such as acid-base mixed oxides, MgO and hydroxyapatites alone have been shown to be able to catalyzed Guerbet reaction often high temperatures are required [1]. Recently Davis et al. applying steady state isotopic transient kinetic analysis (SSITKA) as well as DRIFT analysis for coupling of ethanol on MgO, ascribed the low turnover frequency of the formation of 1-butanol to slow dehydrogenation of ethanol to ethanal over MgO [2].

Table A4

Physicochemical properties of AEMO supported on CNF.

	BET surface (m ² g ⁻¹)	Pore volume (cm ³ g ⁻¹)	CO ₂ uptake (μmol CO ₂ g ⁻¹ catalyst)
CNF	185–216 ^a	0.39–0.43 ^a	n.d.
MgO/CNF	144	0.35	231
BaO/CNF	153	0.33	407 ^b

^a CNF batch having BET surface area of 185 m² g⁻¹ and pore volume of 0.39 cm³ g⁻¹ was used for preparation of MgO/CNF for BaO/CNF batch was used having BET surface area of 216 m² g⁻¹ and pore volume of 0.43 cm³ g⁻¹.

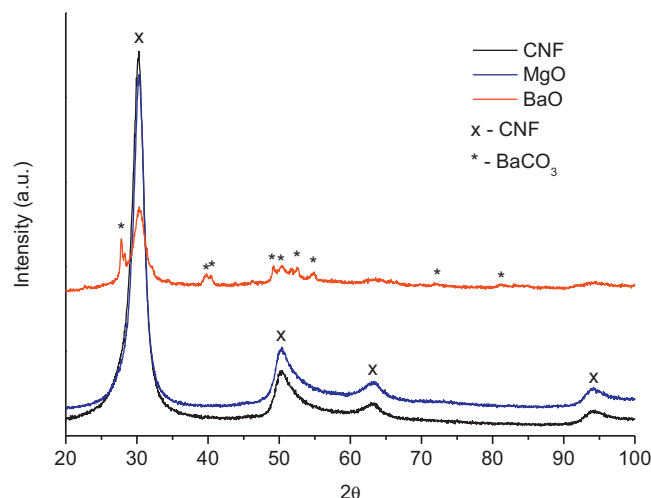
^b Freshly calcined sample of BaO/CNF adsorbed only 245 μmol CO₂ g⁻¹.

There are few examples in the literature employing bifunctional metal–base or metal–acid–base catalysts for Guerbet reaction. Studies focus mainly on the comparison between different metals (Ru, Rh, Pd, Pt, Ag, Ni) supported on a selected support such as Al₂O₃ and MgAlO. Also metals are used in a physical mixture with bases such as K₃PO₄, K₂CO₃ for the production of Guerbet alcohols [3–7]. All of these catalytic systems are mainly tested under liquid-phase conditions and autogenous pressure.

Characterization results

AEMO supported on CNF. Table A4 describes the surface area, pore volume and number of base sites as determined by CO₂ chemisorption for MgO and BaO supported on CNF. Upon impregnation surface area is decreased by 40 m² g⁻¹ accompanied by a slight decrease of pore volume. Overall the number of base sites as determined by CO₂ chemisorption is higher in case of BaO supported on CNF than in case of MgO. Even though same molar amount of base was supported on CNF there is a quite large discrepancy in the amount of base sites, discrepancy for which we at the moment do not have a good explanation.

According to XRD analysis (Fig. A1) in case of MgO/CNF no other crystalline phase has been identified besides diffractions belonging to CNF at 32, 52, 63 and 94 2θ degrees. This may be caused by small particles size as it is generally known that XRD cannot detect crystalline particles smaller than 4 nm. Other possible solution is that MgO is amorphous. In case of BaO/CNF, due to higher weight percentage, however same molar amount of base was supported on CNF, diffractions belonging to CNF were lower in intensity. In addition we see crystalline diffractions belonging to BaCO₃ instead of BaO (Fig. A1), even though precautions have been taken to avoid contact with atmosphere during XRD characterization. Again it does not mean that BaO is not present on CNF, either the BaO crystalline nanoparticles are too small or amorphous.

**Fig. A1.** XRD results of CNF, MgO and BaO supported on CNF.

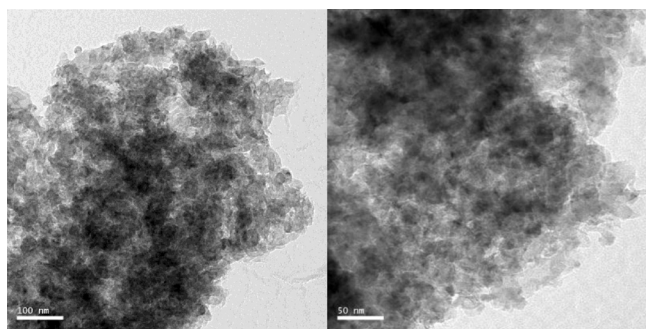


Fig. A2. TEM image of MgO/CNF (left) and BaO/CNF (right).

Table A5

N_2 -physisorption results of copper supported on CNF.

	BET surface ($m^2 g^{-1}$)	Pore volume ($cm^3 g^{-1}$)
CNF	203	0.47
Cu/CNF	210	0.42

Fig. A2 depicts the representative TEM images of MgO and BaO supported on CNF from which particle size distribution has been obtained as can be seen in **Fig. A3**. Particle size distribution is based on counting 100 particles from 3 to 5 different TEM images. In case of MgO the particle size distribution as depicted in **Fig. A2** is broader. This might be explained by the fact that the contrast between corresponding MgO particles and CNF is lower than in the case of BaO and CNF.

Copper supported on CNF. Based on N_2 physisorption analysis of Cu supported on CNF (**Table A5**) there is very low decrease in surface area and pore volume upon impregnation of Cu nitrate on CNF. Slight increase in surface area of Cu/CNF sample can be attributed to experimental error.

From the XRD analysis, not shown, no other diffractions have been found expect diffractions belonging to CNF as Cu/CNF was reduced at 350 °C under flowing H_2 without the usual activation at 600 °C as applied for AEMO supported on CNF.

In **Fig. A4** a representative TEM image of Cu supported on CNF is shown as prepared by incipient wetness impregnation from corresponding nitrates. In **Fig. A5** resulting particles size distribution

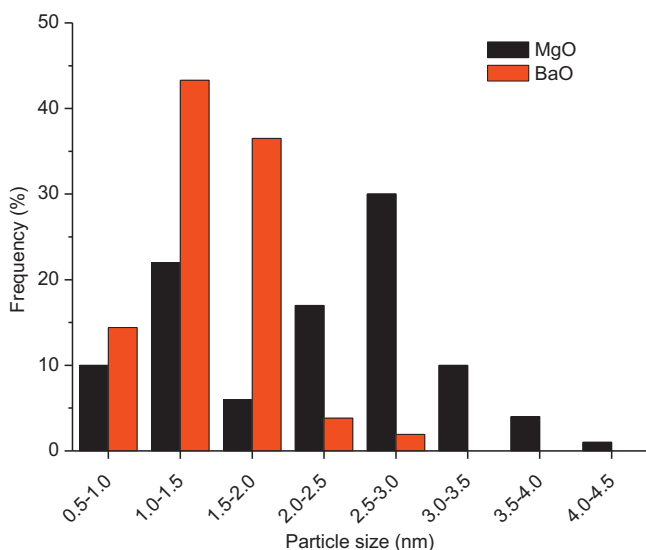


Fig. A3. Particle size distribution of MgO and BaO determined from TEM images shown in **Fig. A2**. Based on counting 100 particles from 3 to 5 different TEM images.

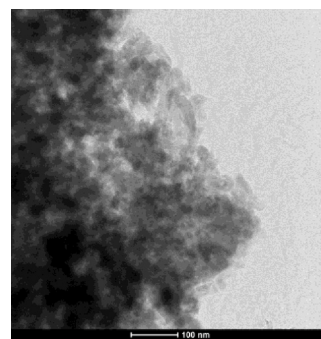


Fig. A4. TEM image of Cu/CNF.

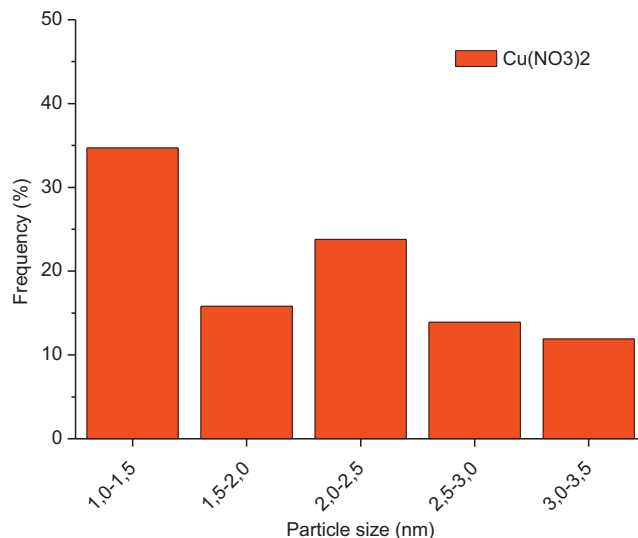


Fig. A5. Particle size distribution of Cu/CNF determined from TEM images shown in **Fig. A4**. Based on counting 100 particles from 3 to 5 different TEM images.

is shown for Cu/CNF based on counting 100 particles from corresponding 3–5 images.

Bifunctional Mg/Cu catalysts supported on CNF. From the N_2 physisorption analysis (**Table A6**), there is a decrease in surface area and pore volume due to impregnation for all three bifunctional Mg/Cu catalyst. Overall, all three catalysts possess quite similar surface area as pore volume.

According to XRD analysis of bifunctional Mg/Cu catalysts (**Fig. A6**) only for sample containing large amount of copper Mg/Cu = 10 diffractions belonging to metallic copper could be identified. This is most probably caused due to high activation temperature applied (600 °C) followed by reduction at 350 °C. For the bifunctional samples containing lower amount of copper no additional copper phases have been found. It is reported that AEMO are good “solvents” for 3d transition metal ions, leading to copper being incorporated in the structure of MgO for samples containing smaller amounts of copper [9].

Table A6

N_2 -physisorption results of bi-functional Mg–Cu supported on CNF.

	BET surface ($m^2 g^{-1}$)	Pore volume ($cm^3 g^{-1}$)
CNF	203	0.47
Mg/Cu = 10	146	0.31
Mg/Cu = 20	145	0.33
Mg/Cu = 30	145	0.30

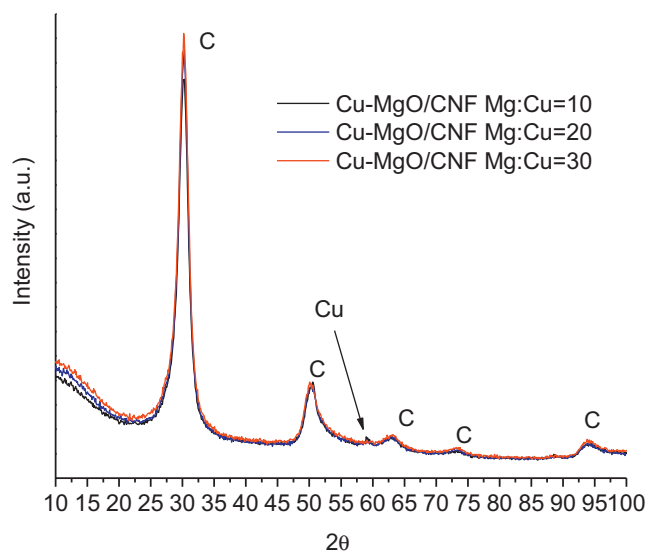


Fig. A6. XRD analysis of bifunctional Mg/Cu catalysts supported on CNF.

Unfortunately for bifunctional Mg/Cu catalysts no CO_2 chemisorption or TEM analysis has been obtained.

List of references used for D1 (also included in the main manuscript reference list).

[1] J.T. Kozłowski, R.J. Davis, ACS Catal. 3 (2013) 1588–1600; W. Ueda, T. Kuwabara, T. Ohshida, Y. Morikawa, Chem. Commun. 1990, 1558–1559; C.A. Hamilton, S.D. Jackson, G.J. Kelly, Appl. Catal. A: Gen. 263 (2004) 63–70; M. León, E. Díaz, S. Ordóñez, Catal. Today 164 (2011) 436–422; E. Hemo, R. Virduk, M.V. Landau, M. Herskowitz, Chem. Eng. Trans. 21 (2010) 1243–1248; M. León, E. Díaz, A. Vega, S. Ordóñez, A. Auroux, Appl. Catal. B Environ. 102 (2011) 590–599; J.I. Di Cosimo, C.R. Apesteguía, M.J.L. Ginés, E. Iglesia, J. Catal. 190 (2000) 261–275; T. Tsuchida, J. Kubo, T. Yoshioka, S. Sakuma, T. Takeguchi, W. Ueda, J. Catal. 259 (2008) 183–189; T. Tsuchida, T. Yoshioka, S. Sakuma, T. Takeguchi, W. Ueda, Ind.

Eng. Chem. Res. 47 (2008) 1443–1452; T. Tsuchida, S. Sakuma, T. Takeguchi, W. Ueda, Ind. Eng. Chem. Res. 45 (2006) 8634–8642; J.I. Di Cosimo, V.K. Díez, M. Xu, E. Iglesia, C.R. Apesteguía, J. Catal. 178 (1998) 499–510; S. Ogo, A. Onda, K. Yanagisawa, Appl. Catal. A: Gen. 402 (2011) 188–195.

[2] T.W. Birky, J.T. Kozłowski, R.J. Davis, J. Catal. 298 (2013) 298, 130–137.

[3] T. Riittonen, E. Toukonniitty, D.K. Madnani, A.-R. Leino, K. Kor-das, M. Szabo, A. Sapi, K. Arve, J. Wärnå, J.-P. Mikkola, Catalysts 2 (2012) 68–84.

[4] I.-C. Marcu, N. Tanchoux, F. Fajula, D. Tichit, Catal. Lett. 143 (2013) 23–30.

[5] R. Miller, G. Bennett, Ind. Eng. Chem. 53 (1961) 33–36.

[6] P. Anbarasan, Z.C. Baer, S. Sreekumar, E. Gross, J.B. Binder, H.W. Blanch, D.S. Clark, F.D. Toste, Nature 491 (2012) 235–239.

[7] A.J. O'Lenick, Jr., US 4767815 (1988).

[8] M.L. Toebes, J.H. Bitter, A.J. van Dillen, K.P. de Jong, Catal. Today 76 (2002) 32–42. M.L. Toebes, Y. Zhang, J. Hajek, A. Nijhuis, J.H. Bitter, J. van Dillen, D.Y. Murzin, D.C. Koningsberger, K.P. de Jong, J. Catal. 226 (2004) 215–225. A.J. Plomp, H. Vuori, A.O.I. Krause, K.P. de Jong, J.H. Bitter, Appl. Catal. A: Gen. 351 (2008) 9–15.

[9] S. Hawkins, Industrial Catalysis: A Practical approach, John Wiley & Sons, 2006.

D.2. Process information

Why go for four reactors?

Thermodynamically it would be favorable to use two reactors to implement the Guerbet reaction. Maintaining the first reactor at a low pressure would favor the dehydrogenation process. While having a second high pressure reactor would favor the hydro-condensation steps (involving aldol condensation, followed by dehydration and finally hydrogenation reactions to higher alcohols). Hence, initially, it was thought that two reactors would be used in the process: the low pressure dehydrogenation reactor and a high pressure hydro-condensation reactor. The ethanol, combined with any other recycled alcohols would react to a mixture of aldehydes, which would be converted to higher alcohols (mostly

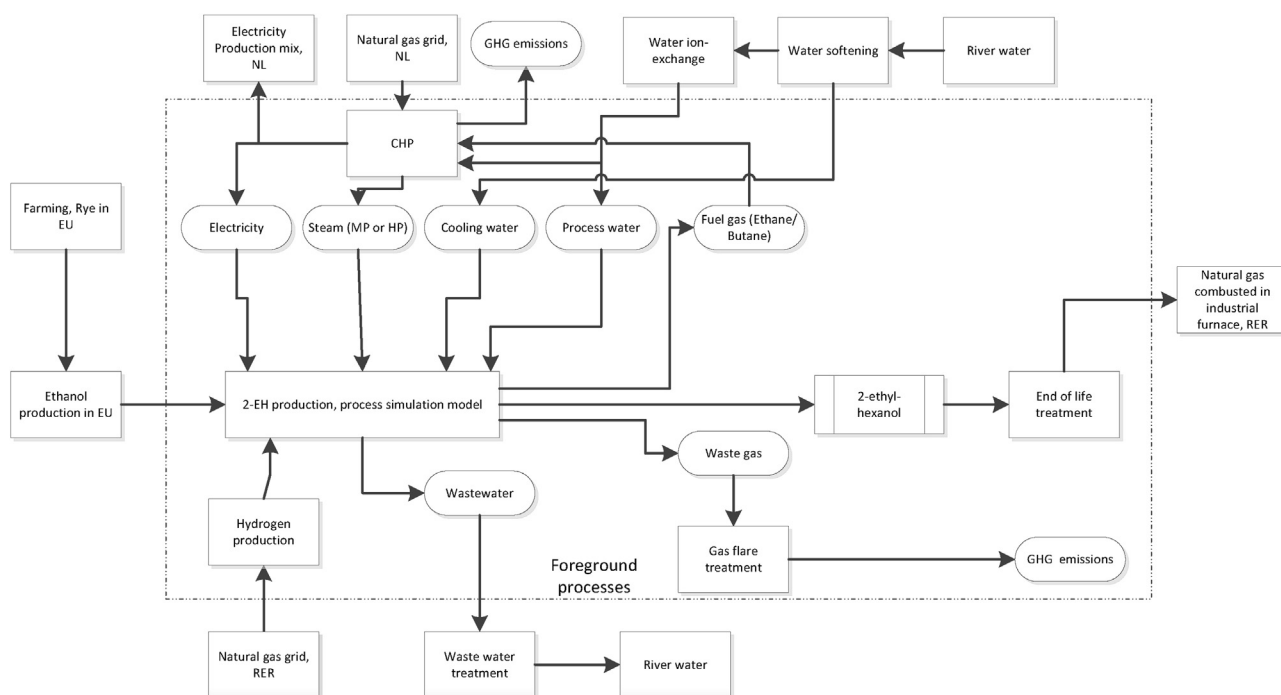


Fig. A7. System diagram showing foreground and background processes for the biobased.

Table A7
Possible side reactions in the hydro-condensation reactor.

#	Reactants	Products	Reaction conversion
1	Butanal + Ethanal + 2H ₂	1-Hexanol + H ₂ O	All ethanal reacts
2	Butanal + Hexanal + 2H ₂	Decanol + H ₂ O	All butanal reacts (if any after 2, 3)
3	Hexanal + Hexanal + 2H ₂	Dodecanol + H ₂ O	All hexanal reacts (if any after 4)
4	Ethanal + Ethanal + 2H ₂	1-Butanol + H ₂ O	All ethanal reacts (if any after 1, 3)
5	Butanal + Butanal + 2H ₂	2-EH + H ₂	All butanal reacts (if any after 2, 3, 4)
6	Ethene + H ₂	Ethane	100%
7	Butene + H ₂	Butane	100%

butanol and 2-EH) in the second reactor. Because mixtures of aldehydes are fed into the second reactor, the amount of by-products can be significant. For this reason, a preliminary study was done where a different configuration using 4 reactors (2 dehydrogenation and 2 hydro-condensation reactors) was tested against the original idea. The reaction conversions that were assumed for this study are as explained in the article. It was found that using the 4-reactor configuration, the theoretical yield is 16% higher than the highest theoretical yield in the 2-reactor configuration, because the first reactor produces only ethanal, giving only butanol in the second reactor, which reacts to only butanal in the third reactor, to form only 2-EH in the fourth reactor, thus avoiding any by-products. In addition, the separations will be significantly easier. Based on this reasoning, it was decided to target the production of 2-EH based on the 4-reactor configuration.

Process model description

The process flow diagram is included in the article (Fig. 7).

The *first process section* is the reaction of ethanol to ethanal (also known as acetaldehyde). The majority of the ethanol reacts in the gas phase to ethanal and hydrogen, but a small fraction forms ethene and water. The water is separated and sent to a wastewater treatment facility. The ethanal, together with hydrogen and some ethene is sent to the next section where the ethanal will form butanol. The ethanol is evaporated and heated to 350 °C and 1 bar, and fed into the reactor. The model reactions, and the assumed reaction conversions are listed in Table 1 in the article. Half the ethanol does not react, and needs to be recycled. Next, the product mixture must be separated. The unconverted ethanol should be recycled, while ethanal and hydrogen will be sent to the next reactor. Water cannot be sent to the next reactor, and it cannot be recycled because it is assumed that it would poison the catalyst. Therefore it must be removed. Ethene stays in the product mixture which is cooled down to 54 °C (dew point), compressed to 2.5 bar, cooled down to its dew point again and fed to the ethanol recovery distillation (column 1.1) which removes ethanol and water from the mixture as a bottom product. The compression stage is used to increase the condenser temperature in the distillation. The higher pressure means that cooling water can be used in the condenser, instead of refrigeration.

It is assumed that water cannot accumulate to much more than 5% in the feed to reactor 101, so water must be removed from the ethanol before the ethanol is recycled. The ethanol water bottom product is close to its azeotropic composition, so a zeolite absorber is used to upgrade the ethanol concentration from 95 wt% to 99.5 wt%. The zeolite is regenerated with ethanol, producing a stream of 30 wt% water, 70 wt% ethanol, which is distilled (column 1.2), producing another ethanol/water azeotropic stream and pure water. The water is sent to a water treatment plant, and the second azeotropic ethanol stream is sent to the same zeolite absorber as the first stream.

The gaseous stream of hydrogen, ethene and ethanal is pressurized with a 3-stage compressor with intercoolers to 23.3 bar. The reason for choosing the value of 23.3 bar is as follows.

Each individual stage has a compression factor of 2.1 (going from 2.5 to 5.3 bar, from 5.3 to 11 and from 11 to 23.3). A decision was made to keep the entire flow in the gaseous state, and to have the outlet temperature close to the practical operating temperature limit of compressors of 170 °C. A higher outlet temperature will increase the investment costs, but reduce the energy consumption of the process because condensation and subsequent re-evaporation steps are omitted. After compression, the stream is heated to 200 °C, and fed into reactor 2.

In the *second process section*, the ethanal reacts to butanol in the first hydro-condensation reactor (reactor 201). The light fractions are removed and hydrogen is recycled. A mixture of butanol and water is sent to the butanol purification section (section 3).

The high pressure reactor converts the ethanal to butanol. The reaction requires an excess of hydrogen of 4 times its stoichiometric requirements in the reactor inlet. The reaction proceeds at a combined partial pressure of hydrogen and ethanal of 20 bar. The reactor temperature is 200 °C. The reactor feed must first be heated to the reactor temperature, but because the reaction is exothermic, the reactor itself requires cooling. Because the reactor operates in plug-flow, the cold reactants cannot be heated by the exothermic reaction. The model reactions and the conversion factors are as listed in Table 1 in the article.

Table A7 shows the possible side reactions in the hydro-condensation reactors (201 and 501). Although these reactions can occur, it should be noted that most of these reactions will not occur in the 4-reactor concept, because the only reactants in the reactor feed are ethanal, hydrogen and ethene.

The reaction product mixture from reactor 201 contains butanol, water, hydrogen and ethane. Butanol and water are condensed. The hydrogen is recycled together with all the ethane, butanol and water that is not removed in the condenser. Because of the high boiling points of butanol and water, only ethane will accumulate in significant amounts.

It was decided to place a purge on the recycle to remove the accumulating ethane. A membrane placed on the purge will recover the hydrogen from the purge stream. The amount of butanol and water in the purge stream is insignificant, and the purge is considered fuel gas (a product) without further treatment.

A sensitivity analysis showed a relation between the butanol losses in the purge, the total heat required in this part of the process and the condenser temperature (which was varied from 0 °C to 160 °C). When we look at an (preliminary, simplified) optimum between heating costs and the butanol yield, ignoring all other economic factors, an economic optimum between butanol losses and heating costs was found at a condenser temperature of 35 °C. This should be investigated in a more elaborate economic analysis in the future. For now, this condenser temperature is used.

Because it is assumed that the partial pressure of hydrogen and ethanal in the reactor inlet must be 20 bar, the total pressure in the reactor becomes 23.3 bar, also taking into account the partial pressures of the recycled ethane, butanol and water.

In section 3, the butanol stream from section 2 is separated into a purified butanol stream, a waste water stream and a fuel gas stream, using start-of-the-art separations. The butanol stream from section 2 contains 19 wt% water, and 2 wt% ethane. Water and ethane are removed from the butanol stream. Water is assumed to poison the catalyst in reactor 401 (section 4), and ethane is removed because it would otherwise accumulate in the recycles in this section. Butanol and water form an azeotrope, and have a wide immiscibility range making this a complicated separation.

Prior to the butanol/water separation, a flash vessel removes a significant part of the ethane. This increases the condenser

temperature in the butanol/water distillations, meaning that cooling water can be used instead of a refrigerated coolant.

The setup of two distillations and a decanter, is based on an earlier research at the Energy research Center of the Netherlands, although some modifications were made due to a different butanol concentration in the flow from the condenser, and the presence of ethane in the system.

The condensed butanol/water stream is sent to a distillation (column 3.1), where butanol is the bottom product, and the butanol/water azeotrope is the top product. This azeotropic mixture is sent to a degasser which allows accumulating ethane to escape from the recycles. A decanter then splits the stream into a butanol rich and a butanol lean (or aqueous) stream. The butanol rich stream is sent back to the first distillation column (column 3.1), while the aqueous stream is sent to a second distillation (column 3.2) where the top product is also the butanol/water azeotrope, and water is the bottom product. Since this top product has almost the same composition as the top product of the first column, it is also degassed and then sent to the same decanter.

The vapor stream from the degasser is cooled to -10°C to remove most butanol and water by condensation. The small butanol/water stream is recycled, and the gas is mixed with other fuel gas streams in section 7 before it is sold.

Section 4 converts the butanol into butanal in the second dehydrogenation reactor of the process. Butanol is removed from the product mixture and is recycled. The butanal, together with the hydrogen, butene and water are compressed and sent to section 5. The butanol stream is heated to its reaction temperature of 350°C , at 1 bar total pressure, and fed into the reactor. The reaction conversions used in the model for the second dehydrogenation reactor (reactor 401) are listed in Table 1 in the article.

The product stream from the reactor contains (on a weight basis) 50% butanol, 44% butanal, 1.2% water, 3.8% butane and 1.2% hydrogen. Butanol should be recycled to reactor 401, and butanal and hydrogen must be sent to reactor 501. When this stream is distilled, butanol will be the bottom product, and a butanal/water azeotrope is the top product together with the even lighter butane and hydrogen. Therefore, contrary to section 3, the butanol is removed from a mixture containing water with only 1 column. It is assumed that although water is a known poison for the catalyst in the second hydro-condensation reactor (reactor 501), the small amount in this stream is not a problem. The amount of water in the feed to reactor 501 is more than 3 times smaller than the amount of water formed in the reaction in that reactor.

Column 4.1 has a partial condenser with a vapor distillate (top) flow. The bottom flow contains (nearly) pure butanol. The top has a very low butanol content (<0.01 wt%), because further downstream (in the 2-EH purification, section 6), butanol can accumulate in a recycle, and will be purged, causing significant product losses. An economic optimization should validate this decision in a future study.

The bottom flow can be recycled directly to the reactor. The distillate flow is compressed to 20 bar, heated to 200°C and fed to the second hydro-condensation reactor (reactor 501).

The dew point temperature of the distillate flow at 20 bar is 160°C , which is only a little below the practical operating limits of many compressors. During the compression, there is a chance that the stream would partially condense. In order to avoid this, a preliminary analysis of the energy consumption of two options resulted in the decision to equip the 2-stage compressor with an intercooler and a separate outlet for a liquid phase. The liquid and vapor streams are pressurized separately. When the streams are recombined they are evaporated.

In section 5, the compressed stream of butanal, after it has been mixed with the excess hydrogen, is fed into the second hydro-condensation reactor (reactor 501). Similar to the conditions in

reactor 501, the reaction requires an excess of hydrogen of 4 times its stoichiometric requirements in the reactor inlet. The final product, 2-EH is formed in reactor 501. The reactions are as given in Table 1 in the article. Just like in section 2, the reaction is exothermic, but the reactor feed must nonetheless be preheated because the reactor operates in plug-flow so the reaction heat cannot be used directly to heat the colder feed flow. The indirect use of the reaction heat through heat integration is considered.

The product stream contains mostly 2-EH, with smaller amounts of water, butane and hydrogen, and trace amounts of butanol. The 2-EH must be purified, while the hydrogen must be recycled. All other components (water and butane) must be removed from both the 2-EH and the hydrogen, either in the condensed phase or from the gaseous recycle. The decision was made to condense all the water and butane together with the 2-EH, and remove them later from the liquid phase. A single stage flash vessel is used to condense the 2-EH, water and butane. An arbitrary choice was made to select a condenser temperature of 60°C . A small purge is included in the design to remove small quantities of light impurities.

In section 6, the product is purified. Water and butane are sent to the water treatment and fuel gas pool respectively. A small purge is required to remove traces of other undesirable materials such as butanol. The condensed stream of 2-EH, water and butane from section 5 can be decanted, producing a water stream that contains so little 2-EH that it is sent straight to the waste water treatment, and a 2-EH stream which still contains some water and all the butane. The water and butane in the 2-EH stream are subsequently removed by distillation.

In the first column, butane is removed as a top product. The second column produces pure 2-EH as a bottom product and a mixture of water and 2-EH as a top product, which is subsequently decanted and split into a water phase and a 2-EH rich phase in a second decanter. The water phase is considered waste water. The 2-EH rich phase is sent back to the distillation column. Because there are de-mixing effects and an azeotrope, it is recommended to investigate the binary system of water and 2-EH in the future, and validate the design decision made with more data. Because there are small quantities butane and butanol still present in the recycle of the 2-EH, two separate bleeds are used. The distillation column produces a small vapor fraction (0.003 wt% is sent to a vapor flow), and in addition, a purge is placed on the recycle to remove butanol.

In process section 7 the outgoing streams are mixed and cooled. The 2-EH product flow is cooled to 30°C . The waste water streams are of roughly the same temperature, so these are mixed before cooling, so that a single larger heat exchanger can be used rather than three smaller heat exchangers. It is assumed that this will reduce investment costs. The waste water stream is cooled to 30°C . The fuel gas streams are also combined. The fuel gas will be burned in a single combined heat and power (CHP) unit, outside the battery limits. A refrigeration unit is included in the capital cost estimate, but this was not a part of the Aspen Plus model. The detailed aspen flowsheet is provided at the end of the appendices and the associated stream tables are provided in an excel file provided as Supporting information.

D.3. Economic analysis

The feedstock and product market prices used for the economic analysis are as stated in Appendix A. Wherever applicable a EUR to USD conversion rate of 1.3 USD/EUR based on June 2011 price levels was used. The costs of utilities and other auxiliaries are reported in Table A8. The refrigeration cost is estimated from the cost of electricity with a co-efficient of performance of 3 [60].

The capital costs for the process equipment were based on data from the SCENT tool developed within the PROSUITE project. In

Table A8

Utility costs.

Utility	Price	Units	Descriptors	Reference
Natural gas	7.5	EUR/GJ	@38.48 MJ/m ³	Eurostat
Electricity	0.1	EUR/kWh		DACE
Steam	27	EUR/ton	@2.26 MJ/kg	DACE
Process water	1	EUR/m ³	demineralized	DACE
Cooling water (river water)	0.05	EUR/m ³	5 °C max heating	DACE
Wastewater treatment	5	EUR/m ³		DACE

DACE: Dutch Association of Cost Engineers (included in references).

Table A9

Process unit costs.

Process unit	Design parameter	Purchased cost (EUR)	Installed cost (EUR)
<i>Reactors</i>			
	<i>Surface area (m²)</i>		
Reactor 101	6263	2,150,042	3,489,122
Reactor 201	1768	585,930	1,133,320
Reactor 401	2782	988,433	1,604,044
Reactor 501	875	355,586	687,783
<i>Columns</i>			
	<i>Product of (height × diameter)</i>		
1.1	226.3	1,126,022	2,048,837
1.2	47.3	316,877	576,568
3.1	148.7	802,662	1,460,474
3.2	16.1	132,368	240,847
4.1	167.2	880,345	1,601,818
6.1	5.3	53,816	97,921
6.2	69.3	431,764	785,609
<i>Reboilers and condensers</i>			
1.1 (reb + cond)		789,784	1,527,619
1.2 (reb + cond)		350,555	678,052
3.1 (reb + cond)		2,353,945	3,820,018
3.2 (reb + cond)		473,432	915,723
4.1 (reb + cond)		627,972	1,214,637
6.1 (reb + cond)		121,302	234,624
6.2 (reb + cond)		334,234	646,483
<i>Heat exchangers – sections</i>			
	<i>Total area needed (m²)</i>		
1	32,272	10,976,273	17,924,085
2	2378	884,044	1,709,938
3	586	386,659	747,884
4	20,440	6,867,890	11,243,376
5	858	424,663	821,392
6	0	0	0
7	192	147,254	284,821
<i>Pumps</i>			
	<i>Power (kW)</i>		
Pump 401 (centrifugal)	3.5	4730	6449
Pump 402 (reciprocating)	26	29,572	74,401
<i>Compressor (single stage)</i>			
	<i>Power (kW)</i>		
Compressor 101 (centrifugal)	2978	4,127,365	6,550,421
Compressor 201 (centrifugal)	16	37,797	59,987
<i>Compressor (multi stage) (excluding intercooler)</i>			
	<i>Power (kW)</i>		
Compressor 102 (centrifugal)	4033	3,123,618	4,957,403
Compressor 401 (centrifugal)	1112	1,700,679	2,699,099
Compressor 402 (centrifugal)	833	1,310,443	2,079,766
<i>Intercoolers</i>			
	<i>Power (kW)</i>		
Intercooler 102a	–37	6503	12,578
Intercooler 102b	–773	41,827	80,904
Intercooler 401a	–4153	225,780	436,708
Intercooler 401b	–867	60,511	117,042
Intercooler 402	–58	6647	12,856
<i>Decanters</i>			
Decanter 301		23,077	38,458
Decanter 601		47,452	79,078
Decanter 602		58,081	96,789
<i>Other process units</i>			
Zeolite	Flow: 14 × 700 dm ³ /s	701,775	932,705
Membrane	Flow: 1.719 Nm ³ /s	1,514,319	1,514,319
Knock-out	<i>h × d</i> 1.5:0.57	6227	10,377
Refrigeration	Power: 4 × 4.75 MW	4,843,295	6,531,139

this tool the installed and purchased equipment costs are based on a number of factors which are specific to each type of equipment.

Table A9 provides design parameters and cost estimates for the various different process units.

Table A10 provides CAPEX for the process.

Table A11 provides an overview of the annual operating expenses for the process. These operating costs are also calculated based on the methodology in the SCENT tool. However, the capital recovery is not included in this OPEX. The raw materials cost includes the cost for ethanol (307 million EUR/year), hydrogen (4.3 million EUR/year) and the catalyst (2.9 million EUR/year). Additional income of 16 million EUR/year is assumed to be derived from sale of co-product fuel gas at 7.5 EUR/GJ. At the designed capacity

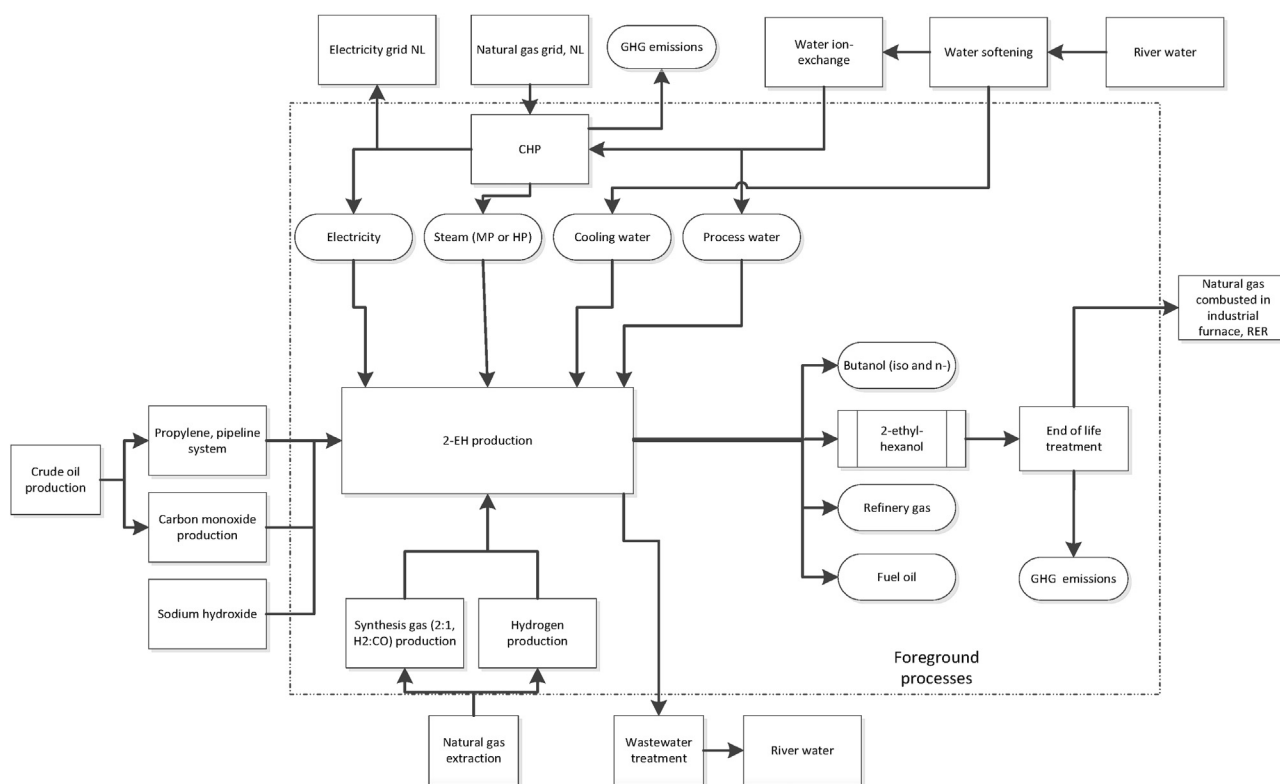


Fig. A8. System diagram showing foreground and background processes for the fossil based system.

Table A10
Overview of capital expenditure.

Component	Estimated cost (€)	Comments
Purchased equipment cost (PEC)	50,431,548	From SCENT
Installed equipment cost 34	81,785,475	From SCENT
Delivery charges (DC)	5,043,155	10% of PEC
Instrumentation and Controls	19,970,893	36% of (PEC + DC)
Buildings incl. services: new plant at new site	22,694,196	45% of PEC
Engineering and supervision	18,306,652	33% of (PEC + DC)
Construction expenses	22,744,628	41% of (PEC + DC)
Legal expenses	5,547,470	10% of (PEC + DC)
Contractor's fee	5,547,470	10% of (PEC + DC)
Contingency	24,408,870	44% of (PEC + DC)
Start-up expenses	14,057,429	From SCENT
Service facilities: rough estimation	28,241,667	51% of (PEC + DC)35
Depreciable capital investment	248,347,905	Sum
Yard improvements: many improvements	5,547,470	10% of (PEC + DC)
Land	3,328,482	6% of (PEC + DC)
Fixed capital investment (FCI)	257,223,858	Sum
Working capital	64,305,964	25% of FCI
Total capital investment (TCI)	321,529,822	Total

the process would produce 2.1 peta joules per year of fuel gas as a co-product. These CAPEX and OPEX form the basis of discounted cash flow analysis over a plant life of 20 years at 10% internal rate of return to yield a minimum viable price for 2-EH at zero net present value.

D.4. LCA assumptions and data inputs

As mentioned in the article, the life cycle of 2-EH produced in a biobased system and a fossil based system have been analyzed. For

Table A11
Overview of operating expenses.

Category	EUR/year
Raw materials cost	314,799,747
Operating labor cost	682,341
Supervision and clerical labor	68,234
Utilities	54,466,377
Maintenance and repairs	26,841,343
Operating supplies	2,684,134
Laboratory charges	68,234
Local taxes	7,716,716
Insurance	2,572,239
Capital recovery	69,551,848
General plant overhead	16,555,151
Administrative costs	136,468
Distribution and marketing	9,623,935
Annual production costs	442,214,919

both the processes a system expansion approach is followed based on ISO standards to give credits for co-products.

Biobased system

The system diagram in Fig. A7 shows the biobased system with the system boundary, background and foreground processes. The processes inside the dotted line are foreground processes which were modeled. The data for remaining processes was mainly based on literature information and databases like Ecoinvent version 2.0. The ethanol is produced from starch containing biomass in EU. In this system a combined heat and power system based on natural gas is used to meet the utility requirements of the process. The CHP is designed to meet the heating requirements for the process and the excess electricity produced as a result is exported to the grid. At the end of life, the 2-EH product is incinerated in a waste incinerator. Based on Li et al., it is assumed that energy recovered is 33% of the lower heating value of 2-EH (40.6 MJ/kg), thus replacing

Table A12
Inventory inputs for production of 1 kg biobased 2-EH.

Parameter	Amount	Unit
<i>Product</i>		
2-EH	1	kg
<i>Avoided product</i>		
Electricity production mix, NL	1.85	kWh
Natural gas high pressure, at consumer, combusted	13.40	MJ
<i>Inputs</i>		
Ethanol, from biomass, RER ^a	1.757	kg
Hydrogen, from natural gas, RER	0.011	kg
Water, decarbonized, RER	670.21	kg
Water, completely softened, RER	6.87	kg
Natural gas high pressure, at consumer	22.03	MJ
<i>Emissions to air</i>		
Water vapor	13.04	kg
Carbon dioxide, fossil	1.813	kg
Dinitrogen monoxide	3.21×10^{-6}	kg
Methane, fossil	6.42×10^{-5}	kg
<i>Emissions to water</i>		
Water, from cooling to river	670.9	kg
Output to wastewater treatment	0.547	kg

NL, Netherlands; RER, Average European context.

^a The CED and GHG emissions associated with ethanol products are based on Patel et al. [2], the CED and GHG emissions associated with the inputs are provided in Appendix A.

Table A13
Mass balance data for updated ESA.

	Step-1			Step-2		Step-3			Step-4	
	Input	Output per pass	Overall output	Input	Overall output	Input	Output per pass	Overall output	Input	Overall output
Ethanol	1000.0	500.0								
Ethanal		430.9	861.8	861.8						
Hydrogen		19.6	39.1	43.5			8.8	17.6	19.6	
Ethene		30.5	61.0	61.0						
Water		19.6	39.1		176.1		8.8	17.6		79.2
Butanol					725.1	725.1	362.5			
Ethane					65.4					
Butanal							317.4	634.9	634.9	
Butene							27.4	54.9	54.9	
2-EH										572.3
Butane										56.9

natural gas. In the case of biobased process this incineration leads to biogenic GHG emissions which do not contribute to climate change.

Table A12 gives the inventory inputs for production of 1 kg of 2-EH system.

Fossil based system

The system diagram in Fig. A8 shows the fossil based system for 2-EH with the system boundary, background and foreground

processes. Similar to the biobased system the processes inside the dotted line are foreground processes. The data for remaining processes was mainly based on literature information and databases like the Ecoinvent version 2.0. The CHP in this case is also modeled similar to the biobased system and runs on natural gas. Also in this case the product is assumed to be incinerated with energy recovery at the end of life. However, being a fossil based product, the GHG emissions from incineration of the product, contribute to climate change. Since the data is based on proprietary and confidential sources, a system inventory for the process can be provided on request. However, the CED and GHG emission values associated with each of the background processes and some of the foreground processes are provided in Appendix E.

Appendix E.

This section includes the assumptions and mass balance data for updated ESA of 2-EH production from biobased and fossil based resources.

As mentioned in the article, the updated ESA for biobased process was based on a four reactor approach and thereby mimicking the processes taking place in the detailed process design. The reactions taking place in the four reactors, conversions and selectivities are as described in Table 1 in the article. Table A13 provides the mass balance which forms the basis of updated ESA for the biobased

process. The fossil based process remains exactly the same as the one for primary ESA.

Appendix F.

Data values associated with graphs.

Figure 9

	Ethane	Ethanal	Propanone	Butanal	Ethylacetate	(2E)-but-1-enal	1-Butanol	2-Ethyl-1-butanol	1-Hexanol	2-Ethyl-2-hexanol	2-Ethyl-1-hexanol	1-Octanol	Other
MgO	0.30	13.84	0.44	3.72	1.52	1.65	46.19	2.53	3.90	–	–	–	25.92
MgO-1h	9.37	33.52	7.42	–	–	4.53	32.53	–	–	–	–	–	12.63
BaO	0.13	15.09	–	2.76	3.59	1.14	43.98	2.35	7.17	1.14	0.73	1.08	20.82
BaO-1h	1.80	52.47	–	–	2.17	–	36.61	–	1.00	–	–	–	5.96

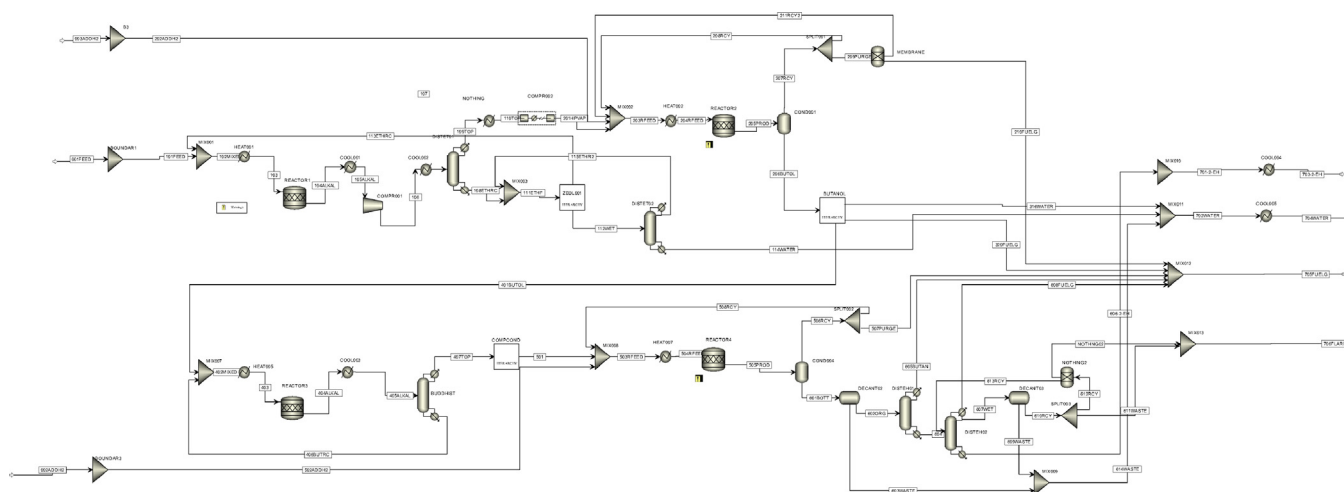
Figure 11

	Methane	Ethane	Ethanal	Propanone	Butanal	Ethylacetate	(2E)-but-1-enal	1-Butanol	2-Ethyl-1-butanol	1-Hexanol	Other
MgO		0.30	13.84	0.44	3.72	1.52	1.65	46.19	2.53	3.90	25.92
Mg/Cu = 10	0.29	0.14	14.57	0.17	2.51	1.86	1.70	47.88	1.64	2.26	26.97
Mg/Cu = 20	0.07	0.41	18.73	0.51	2.39	1.40	1.68	48.92	0.96	1.96	22.98
Mg/Cu = 30	0.64	0.11	8.61		3.99	–	2.30	45.87	3.38	3.19	31.92

Figure 12

	Ethanol	Propanone	Butanal	1-Butanol	1-Hexanol	Other	Conversion
MgO-1h	18.21			52.27		29.52	1.21
MgO-5h	21.12			50.33		28.55	0.38
PM(MgO + Cu)-1h	56.18	1.46	6.45	29.66	1.86	4.40	18.78
PM(MgO + Cu)-5h	61.32	2.73	3.84	26.33	0.96	4.82	11.05

The Aspen flowsheet is shown below, including all the names of the streams. The names of the streams in the mass balance file (Excel file) correspond with this figure. Please zoom in for better visibility of the figure.

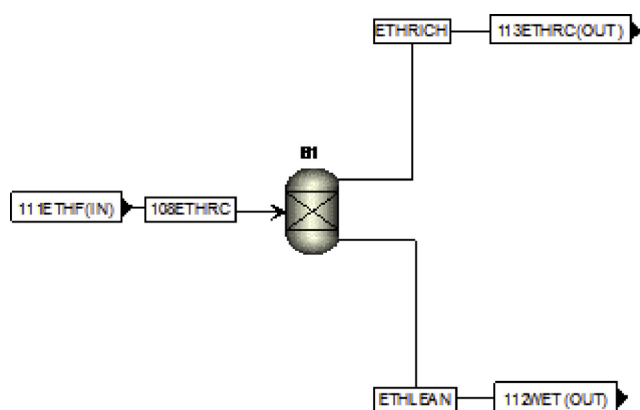


Remarks

The model contains three subsections (hierarchy), called ZEO-LITE, BUTANOL and COMPCOND. These are the zeolite absorber for the ethanol purification, the butanol/water separation and the butanal compression with partial condensation respectively. The flow sheets of the three subsections are shown on the next page and the respective stream tables can be found in the excel file which is provided as Supporting information.

The model contains several streams and units that are called “nothing” or variations to that word. These are all very small streams, bypassing a loop, to avoid convergence problems of the model. One is visible in the flow sheet above, and

Zeolite hierarchy



The PFD illustrates the process flow for a distillation system. It begins with an input stream 407(TOP(IN)) entering distillation column 407. The overhead product of column 407 passes through a compressor (COMPR003) and a knockout drum before entering distillation column 408(VAP). The bottom product of column 408 (411) is sent to a mixer (MIX008). The side product of column 408 (408LIQ) is sent to a pump (PUMP001). The overhead product of column 408 (412) is sent to a mixer (MIX006). The bottom product of column 408 (413) is sent to a reboiler (HEAT006). The reboiler (HEAT006) is heated by a heat source (501) and its output (501(OUT)) is sent to a final output stream (501(OUT)).

[illegible]

Supplementary data associated with this article can be found, in the online version, at <http://dx.doi.org/10.1016/j.cattod.2014.03.070>.

- [1] P.T. Anastas, *Green Chemistry: Theory and Practice*, Oxford University Press, Oxford, 1998.
- [2] A.D. Patel, K. Meesters, H. den Uil, E. de Jong, K. Blok, M.K. Patel, Sustainability assessment of novel chemical processes at early stage: application to biobased processes, *Energy Environ. Sci.* 5 (2012) 8430.
- [3] H. Sugiyama, Decision-making Framework for Chemical Process Design Including Different Stages of Environmental, Health and Safety (EHS) Assessment, 2007.
- [4] J.J. Bozell, G.R. Petersen, Technology development for the production of biobased products from biorefinery carbohydrates-the US Department of Energy's Top 10 revisited, *Green Chem.* (2010) 539.
- [5] J. Lane, *Biofuels Digest* (2013).
- [6] P. Anex Robert, L. Ogletree Alison, Life-cycle assessment of energy-based impacts of a biobased process for producing 1,3-propanediol, in: *Feedstocks for the Future*, American Chemical Society, Washington, DC, 2006, pp. 222–238.
- [7] M. Patel, C. Bastioli, L. Marini, E. Wurdinger, Life-cycle assessment of bio-based polymers and natural fiber composites, in: *Biopolymers Online*, Wiley-VCH Verlag GmbH & Co. KGaA, Weinheim, 2005.
- [8] B. Hermann, K. Blok, M. Patel, Producing bio-based bulk chemicals using industrial biotechnology saves energy and combats climate change, *Environ. Sci. Technol.* 41 (2007) 7915–7921.
- [9] J.E.A. Seabra, I.C. Macedo, H.L. Chum, C.E. Faroni, C.A. Sarto, Life cycle assessment of Brazilian sugarcane products: GHG emissions and energy use, *Biofuels Bioprod. Biorefining* 5 (2011) 519–532.
- [10] OECD-FAO, *Agricultural Outlook 2011–2020*, 2012.

- [11] A. Eisentraut, Sustainable Production of Second Generation Biofuels Potential and Perspectives in Major Economies and Developing Countries, 2010.
- [12] J.A. Posada, A.D. Patel, A. Roes, K. Blok, A.P.C. Faaij, M.K. Patel, Potential of bioethanol as a chemical building block for biorefineries: preliminary sustainability assessment of 12 bioethanol-based products, *Bioresour. Technol.* 135 (2013) 490–499.
- [13] G. Knothe, Synthesis, applications, and characterization of Guerbet compounds and their derivatives, *Lipid Technol.* 14 (2002) 101–104.
- [14] A. Ndou, N. Coville, Self-condensation of propanol over solid-base catalysts, *Appl. Catal. A: Gen.* 275 (2004) 103–110.
- [15] M. Guerbet, Branched aldol alcohols, *C. R. Acad. Sci. Paris* 128, 511 (1899) 5.
- [16] C. Yang, Z.Y. Meng, Bimolecular condensation of ethanol to 1-butanol catalyzed by alkali cation zeolites, *J. Catal.* 142 (1993) 37–44.
- [17] H. Bahrmann, H. Hahn, D. Mayer, 2-Ethylhexanol, in: *Ullmann's Encyclopedia of Industrial Chemistry*, Wiley-VCH Verlag GmbH & Co. KGaA, Weinheim, 2000.
- [18] S. Both, G. Fieg, E. Reuter, F. Bartschick, B. Gutsche, Method for producing Guerbet alcohols. US 6911567 (2005).
- [19] E. Scherf, H. Letsch, C. Schroder, A. Herrmann, Method for producing metal-free Guerbet alcohols. US 6419797 (1999).
- [20] G. Mueller, B. Gutsche, L. Jeromin, U. Steinberner, R. Sedelies, R. Bohlander, R. Ridinger, D. Springer, F. Buettgen, F. Bartschik, Process for the production of Guerbet alcohols. US 5777183 (1998).
- [21] J.E. Yates, Process for condensation of alcohols. US 3979466 (1976).
- [22] J.E. Yates, Process for condensation of alcohols. US 3917722 (1975).
- [23] C.A. Hamilton, S.D. Jackson, G.J. Kelly, Solid base catalysts and combined solid base hydrogenation catalysts for the aldol condensation of branched and linear aldehydes, *Appl. Catal. A: Gen.* 263 (2004) 63–70.
- [24] J.T. Kozlowski, R.J. Davis, Heterogeneous catalysts for the Guerbet coupling of alcohols, *ACS Catal.* 3 (7) (2013) 1588–1600.
- [25] H. Hattori, Heterogeneous basic catalysis, *Chem. Rev.* 95 (1995) 537–558.
- [26] M.A. Landau, V.V. Shchekin, Difference in mechanisms of dehydrogenation on oxides and metals. *Bull. Acad. Sci. USSR* 9 (1960) 885–887.

- [27] W. Ueda, T. Kuwabara, T. Ohshida, Y. Morikawa, A low-pressure Guerbet reaction over magnesium oxide catalyst, *J. Chem. Soc. Chem. Commun.* (1990) 1558–1559.
- [28] M. Leon, E. Diaz, S. Ordonez, Ethanol catalytic condensation over Mg–Al mixed oxides derived from hydrotalcites, *Catalysis Today* 164 (2011) 436–442.
- [29] E. Hemo, R. Virduk, M.V. Landau, M. Herskowitz, Biogasoline and high alcohols production by one step ethanol conversion on densified MgO catalyst with enhanced concentration of surface active sites, *Chem. Eng.* 21 (2010).
- [30] M. Leon, E. Diaz, A. Vega, S. Ordonez, A. Auroux, Consequences of the iron–aluminium exchange on the performance of hydrotalcite-derived mixed oxides for ethanol condensation, *Appl. Catal. B: Environ.* 102 (2011) 590–599.
- [31] J. Di Cosimo, C. Apesteguia, M. Gines, E. Iglesia, Structural requirements and reaction pathways in condensation reactions of alcohols on Mg_xAlO_x catalysts, *J. Catal.* 190 (2000) 261–275.
- [32] T. Tsuchida, J. Kubo, T. Yoshioka, S. Sakuma, T. Takeguchi, W. Ueda, Reaction of ethanol over hydroxyapatite affected by Ca/P ratio of catalyst, *J. Catal.* 259 (2008) 183–189.
- [33] T. Tsuchida, T. Yoshioka, S. Sakuma, T. Takeguchi, W. Ueda, Synthesis of biogasoline from ethanol over hydroxyapatite catalyst, *Ind. Eng. Chem. Res.* 47 (2008) 1443–1452.
- [34] T. Tsuchida, S. Sakuma, T. Takeguchi, W. Ueda, Direct synthesis of n-butanol from ethanol over nonstoichiometric hydroxyapatite, *Ind. Eng. Chem. Res.* 45 (2006) 8634–8642.
- [35] J. Di Cosimo, V. Diez, M. Xu, E. Iglesia, C. Apesteguia, Structure and surface and catalytic properties of Mg–Al basic oxides, *J. Catal.* 178 (1998) 499–510.
- [36] S. Ogo, A. Onda, K. Yanagisawa, Selective synthesis of 1-butanol from ethanol over strontium phosphate hydroxyapatite catalysts, *Appl. Catal. A: Gen.* 402 (2011) 188–195.
- [37] T.W. Birkly, J.T. Kozlowski, R.J. Davis, Isotopic transient analysis of the ethanol coupling reaction over magnesia, *J. Catal.* 298 (2013) 130–137.
- [38] T. Riittonen, E. Toukonen, D.K. Madhani, A. Leino, K. Kordas, M. Szabo, A. Sapi, K. Arve, J. Wärnå, J. Mikkola, One-pot liquid-phase catalytic conversion of ethanol to 1-butanol over aluminium oxide—the effect of the active metal on the selectivity, *Catalysts* 2 (2012) 68–84.
- [39] I. Marcu, N. Tanchoux, F. Fajula, D. Tichit, Catalytic conversion of ethanol into butanol over M–Mg–Al mixed oxide catalysts (M = Pd, Ag, Mn, Fe, Cu, Sm, Yb) obtained from LDH precursors, *Catal. Lett.* 143 (2013) 23–30.
- [40] R. Miller, G. Bennett, Producing 2-ethylhexanol by the Guerbet reaction, *Ind. Eng. Chem.* 53 (1961) 33–36.
- [41] P. Anbarasan, Z.C. Baer, S. Sreekumar, E. Gross, J.B. Binder, H.W. Blanch, D.S. Clark, F.D. Toste, Integration of chemical catalysis with extractive fermentation to produce fuels, *Nature* 491 (2012) 235–239.
- [42] A.J. O'Lenick Jr., Guerbet alcohol esters. US 4767815 (1988).
- [43] A.D. Patel, K. Meesters, H. den Uil, E. de Jong, E. Worrell, M.K. Patel, Early-stage comparative sustainability assessment of new bio-based processes, *ChemSusChem* 6 (2013) 1724–1736, <http://dx.doi.org/10.1002/cssc.201300168>.
- [44] M.L. Toebes, J.H. Bitter, A.J. Van Dillen, K.P. de Jong, Impact of the structure and reactivity of nickel particles on the catalytic growth of carbon nanofibers, *Catal. Today* 76 (2002) 33–42.
- [45] M.L. Toebes, Y. Zhang, J. Håjek, T. Alexander Nijhuis, J.H. Bitter, A. Jos Van Dillen, D.Y. Murzin, D.C. Koningsberger, K.P. de Jong, Support effects in the hydrogenation of cinnamaldehyde over carbon nanofiber-supported platinum catalysts: characterization and catalysis, *J. Catal.* 226 (2004) 215–225.
- [46] A.J. Plomp, H. Vuori, A.O.I. Krause, K.P. de Jong, J.H. Bitter, Particle size effects for carbon nanofiber supported platinum and ruthenium catalysts for the selective hydrogenation of cinnamaldehyde, *Appl. Catal. A: Gen.* 351 (2008) 9–15.
- [47] Aspen Technology, Aspen Plus v7.3. 7.3 (2011–2012).
- [48] B. Linnhoff, V. Sahdev, Pinch technology, in: Ullmann's Encyclopedia of Industrial Chemistry, Wiley-VCH Verlag GmbH & Co. KGaA, Weinheim, 2000.
- [49] Abengoa Bioenergy, Abengoa Bioenergy Netherlands, 2013.
- [50] S.Y. Ereev, M.K. Patel, Standardized cost estimation for new technologies (SCENT) methodology and tool, *J. Bus. Chem.* 9 (2012) 31.
- [51] ICIS, CW Price Reports, Chemical Week (2007–2011).
- [52] Alibaba group, Chemicals (www.alibaba.com/chemicals.p8), 2011.
- [53] World Association of Beet and Cane Growers, Flashmarkets, 2011.
- [54] Dutch Association of Cost Engineers, DACE prijzenboekje, 28th ed., Dutch Association of Cost Engineers, Nijkerk, The Netherlands, 2011.
- [55] Eurostat, Natural gas prices for industrial consumers with annual consumptions between 10000 and 100000 GJ, 2012.
- [56] D. Humbrid, R. Davis, L. Tao, C. Kinchin, D. Hsu, A. Aden, P. Schoen, J. Lukas, B. Olthof, M. Worley, D. Sexton, D. Dudgeon, Process Design and Economics for Biochemical Conversion of Lignocellulosic Biomass to Ethanol: Dilute-Acid Pretreatment and Enzymatic Hydrolysis of Corn Stover. NREL/TP-5100-47764, 2011.
- [57] Pre Consultants, SimaPro-Ecoinvent database. 7.3, 2011.
- [58] European Union, DIRECTIVE 2009/28/EC OF THE EUROPEAN PARLIAMENT AND OF THE COUNCIL of 23 April 2009 on the promotion of the use of energy from renewable sources and amending and subsequently repealing Directives 2001/77/EC and 2003/30/EC, 2009.
- [59] D. Mu, T. Seager, P. Rao, F. Zhao, Comparative life cycle assessment of lignocellulosic ethanol production: biochemical versus thermochemical conversion, *Environ. Manage.* 46 (2010) 565–578.
- [60] M.K. Patel, M. Crank, V. Dornburg, B. Hermann, L. Roes, B. Hüsing, L. Overbeek, F. Terragni, E. Recchia, Medium and long-term opportunities and risks of the biotechnological production of bulk chemicals from renewable resources, 2006.
- [61] L. Shen, E. Worrell, M.K. Patel, Comparing life cycle energy and GHG emissions of bio-based PET, recycled PET, PLA, and man-made cellulose, *Biofuels Bioprod Biorefining* 6 (2012) 625–639.
- [62] M.A. Huijbregts, S. Hellweg, R. Frischknecht, H.W. Hendriks, K. Hungerbühler, A.J. Hendriks, Cumulative energy demand as predictor for the environmental burden of commodity production, *Environ. Sci. Technol.* (2010) 2189.
- [63] S. Solomon, D. Qin, M. Manning, Z. Chen, M. Marquis, K.B. Averyt, M. Tignor, H.L. Miller, The Physical Science Basis. Contribution of Working Group I to the Fourth Assessment Report of the Intergovernmental Panel on Climate Change, 2007, pp. 211.
- [64] M. Weiss, J. Haufe, M. Carus, M. Brandão, S. Bringezu, B. Hermann, M.K. Patel, A review of the environmental impacts of biobased materials, *J. Ind. Ecol.* 16 (2012) S169–S181.
- [65] L.M. Tufvesson, P. Tufvesson, J.M. Woodley, P. Borjesson, Life cycle assessment in green chemistry: overview of key parameters and methodological concerns, *Int. J. Life Cycle Assess.* 18 (2013) 431–444.
- [66] A.M. Frey, J. Yang, C. Feche, N. Essayem, D.R. Stellwagen, F. Figueras, K.P. de Jong, J.H. Bitter, Influence of base strength on the catalytic performance of nano-sized alkaline earth metal oxides supported on carbon nanofibers, *J. Catal.* 305 (2013) 1–6.
- [67] S. Kim, B.E. Dale, Indirect land use change for biofuels: testing predictions and improving analytical methodologies, *Biomass Bioenergy* 35 (2011) 3235–3240.
- [68] B. Wicke, P. Verweij, H. van Meijl, D.P. van Vuuren, A.P. Faaij, Indirect land use change: review of existing models and strategies for mitigation, *Biofuels* 3 (2011) 87–100.
- [69] A. Chauvel, G. Lefebvre, Petrochemical Processes (Volume 1: Synthesis-Gas Derivatives and Major Hydrocarbons), Editions Technip, Paris, France, 1989.
- [70] A. Chauvel, G. Lefebvre, Petrochemical Processes (Volume 2: Major Oxygenated, Chlorinated, and Nitrated Derivatives), Editions Technip, Paris, France, 1989.